ADDIS ABABA INSTITUTE OF TECHNOLOGY

SCHOOL OF GRADUATE STUDIES

SCHOOL OF CIVIL AND ENVIRONMENTAL ENGINEERING

” Parametric Study on the Influence of Tunneling on Adjacent Deep Foundation”

By: Kalkidan Gashaw

A THESIS SUBMITTED TO THE SCHOOL OF GRADUATE STUDIES, ADDIS ABABA UNIVERSITY, IN PARTIAL FULFILLMENT OF THE REQUIREMENTS FOR THE DEGREE OF MASTERS OF SCIENCE IN CIVIL ENGINEERING [GEOTECHNICAL ENGINEERING]

Advisor: Dr.-Ing. Henok Fikre

September, 2021

School of Graduate Studies
School of Civil and Environmental Engineering

Parametric Study on the Influence of Tunneling on Adjacent Deep Foundation

By:Kalkidan Gashaw

Thesis Submitted to School of Graduate Studies in Partial Fulfillment of the Requirement for Degree of Master of Science in Geotechnical Engineering

Approved by Board of Examiners

Dr.-Ing .Henok Fikre	_____	_____
Advisor	signature	Date
_____	_____	_____
Internal examiner	signature	Date
_____	_____	_____
External Examiner	signature	Date
_____	_____	_____
Chairman	signature	Date

Declaration

I, the undersigned, declare that this thesis is my original work performed under the supervision of my research advisor **Dr.-Ing.Henok Fikre** and has not been presented as a thesis for a degree in any other university. All sources of materials used for this thesis have been duly acknowledged.

Name: KALKIDAN GASHAW

Signature: _____

Place Institute of Technology

Addis Ababa University

Addis Ababa.

Date: _____

Acknowledgements

Compilation of this thesis has taken me through a journey longer than I expected at first. Thanks to the Lord it has now made it to the final stages.

I thank my advisor, **Dr.-Ing.Henok Fikre** (Civil Engineering Geotechnical Department, Addis Ababa Institute of Technology) for his availability for supervision and for his advices during my research work.

I am also indebted to Addis Ababa University Female scholarship program for giving me this opportunity to learn in the Master's program in Addis Ababa Institute of Technology. Many

Friends and family members have played a great role in helping me with moral support and also technical advices. Therefore, I appreciate all they have done for having been at constant disposal for encouragement and advices whenever I needed them.

Abstract

Numerous high rise buildings are supported by deep foundations in major cities or urban areas. Due to the rapid increasing demand for infrastructures construction in congested urban areas, tunnels are often preferred for under ground transportation. The construction of tunnels are close to some existing piles foundations will affect pile capacity and stability due to soil deformation caused by vertical and horizontal movement, which changes the axial load distribution along the piles.

In this study, the effect of a 6m open face advancing tunnel on a three by three group pile in c- ϕ soil has been investigated using three dimensional finite element analysis software (PLAXIS 3D). Hardening soil (HS) constitutive model and isotropic elastic model for piles, pile cap, tunnel lining, and tunnel boring machine (TBM) were used for analysis. A parametric study has been carried out to investigate the behavior of piles through varying ratios of tunnel depth (H) to tunnel diameter (D) (namely H/D= 2.0, 2.5, and 3.0).

From the analysis result, the factor of safety of the pile was reduced from 3.0 to1.62 due to tunnel advancement 2m near to the pile tip, large pile settlement was observed when the tunnel face below the pile tip(H/D=3.0). And also the load carrying capacity of the pile at the base significantly decreases. In addition, skin friction of the pile was significantly decreased when the tunnel approaches to the shaft of the pile.

Contents

List of Figures

List of Table

LIST OF SYMBOLS:

C = Cohesion of Soil (kN/m^2)

φ = Angle of Internal Friction of Soil (Degree)

ψ = Dilatancy Angle of Soil (Degree)

γ = Bulk Density of Soil (kN/m^3)

E = Young's Modulus of Elasticity of Soil (kN/m^2)

ν= Poisson's Ratio of Soil

D = diameter of tunnel (m)

H = Depth of tunnel (m)

K_0 = Earth Pressure Coefficient At Rest

K_a = Active Earth Pressure Coefficient

K_p = Passive Earth Pressure Coefficient

σ_v = Total Vertical Pressure (kN/m^2)

σ_h = Total Horizontal Pressure (kN/m^2)

β = Inclination Angle of the Backfill to the Horizontal

q = Ultimate Bearing Capacity of Soil (kN/m^2)

N_c, N_q, N_γ = Bearing Capacity Coefficients

D_w = Depth of Water Table below Ground Surface (m)

D = diameter of pile

E_{ref}^{50}- Reference secant modulus of elasticity

E_{ref}^{oed}- Tangent stiffness for primary odometer loading

E_{ref}^{ur}- Unloading/ Reloading stiffness

S = surface settlement at a transverse distance x from the tunnel centre line

S_{max}= maximum settlement at x=0

i = location of maximum settlement gradient or point of inflexion.

V_L= ground loss

CHAPTER ONE

1. Introduction

1.1 General Background

In recent years, there has been a rise in infrastructure development in highly populated or urban areas. Transportation plays a significant role to facilitate the people to move from one place to other. To satisfy the demand for transportation in the populated area several projects are under taken including road, rail transport on flyovers and underground tunnels. For the case of lack of space in urban areas the underground structure demands are increased. This resulted tunnel excavation adjacent to existing building foundations. Different transportation and utility tunnels are excavated near to existing building foundations and bridge structures. When the foundations are deep, proper consideration of the deformations induced by tunnel excavation.

This causes the pile axial responses like bearing capacity and settlement due to the vertical and horizontal movement of soil near to the pile (Chiang and Lee (2007)). It also causes bending moment and deflection of the foundation. It's also important to review the influence of tunneling operations on the adjacent piles in terms of additional stresses and displacements of those piles to manage the damaging settlements of those piles.

Chen et al. (1999) reported the effect of tunneling on pile foundation are difficult to understand because of different parameters like working load of pile, tunnel depth to diameter ratio, the size and relative position of tunnel. In addition to that tunnel advancement causes some level of impact on adjacent foundation.

In solving geotechnical problems, practicing engineers and researchers use different methods to come up with effective and reliable solutions. Among the methods experimental procedures has been widely employed. Although the method has been used to solve certain problems, it require complex laboratory setup in studying large scale geotechnical problems, such as tunneling, slop stability, pile and etc. beside the complexity of resources and time experimental method is exposed to human and equipment errors. On the other hand researchers also used limit equilibrium method to tackle problems encountered in geotechnical engineering. Despite of the fact that the method is effective in some problems, it requires to make un realistic assumptions

and material behavior. In recent years, following the advancement of computer technology a numerical solution such as Finite Element Method (FEM) has been widely employed in solid and soil mechanics Ghazavi ME, Amir (2008). The method is powerful and effective in solving complex and large scale geotechnical problems.

1.2 Statement of the Problem

To meet the demand for infrastructures in the populated area, several projects are undertaken. For instance road, railway, and underground tunnels are common projects in the geographic region**.** But transportation numerous utility lines are used below the bottom level of the ground. Especially in highly populated or congested urban areas tunnel excavation adjacent to the high-rise buildings are usually observed. These tunnel excavations below ground level result in relaxation of in-situ stress i.e. ground loss**.** The ground loss intern affects the behavior of the adjacent building foundation system. Hence this study merely focuses on assessing the bending moment and deformation behavior of deep foundation influenced by adjacent tunnel excavation. parametric study carried out varying tunnel excavation through the ratio of tunnel depth (H) to tunnel diameter (D)

1.3 Research Questions

- How does the tunnel excavation affect the load transfer mechanism of existing piles?
- How does the tunnel excavation influence the load carrying capacity of the existing pile?
- Where does the larger differential settlement of the existing pile occur?
- Does the relative location of the tunnel excavation effect skin friction of the existing pile?
- Does the factor of safety of the existing pile affected by the relative position of the tunnel lining?

1.4 Objectives

1.4.1General Objective

➢ The overall objective of this research is to investigate the behavior of piles influenced by tunnel excavation.

1.4.2Specific Objectives

➢ The above general is achieved by addressing the following specific objectives.

- Investigate load sharing mechanism of the existing piles due to the tunnel excavation.
- Study the reduction of skin friction of the exiting pile as a result of tunnel excavation.
- Conduct parametric study and estimate pile group settlements through varying relative position of the tunnel excavation.
- Explore load caring capacity and factor of safety of the pile group due to the nearby tunnel excavation.
- Examine the differential settlements of the existing pile as a result of the tunnel excavation.
- Determine the influence zone of the tunnel excavation around the pile group.

1.5 Significance of the Study

Researchers and practitioners can potentially benefit from the output of this research work

- To understand influences of the tunneling excavation on the existing pile foundation.
- To have a better attention given for existing pile foundation by designers & practicing engineers.
- To have a better prediction on the settlement and deformation effect on the existing pile.

1.6 Research Scope

Although the scope of the study area is vast, it is difficult to cover all in this study due to time and resource limitations. Hence, it is very crucial to limit the study area according to the given resource and time. Accordingly, Vibrations (dynamic loads) induced during the excavation will not be considered. And also the horizontal distance between tunnel and piles will be constant.

1.7 Methodology

First, the effect of tunnel excavations with adjacent deep foundation settlements is studied. The parameters soil, tunnel, and pile structures are obtained from previously done researches. Then, representative properties for c-ϕ soil are taken and used as input in modeling the tunnel excavation and loading scenarios. Group pile is used for modeling and the tunnel construction is

assuming by tunnel boring machine (TBM) advancement (Chapman, 2010). The depth of tunnel excavation is varied based on the ratio of tunnel depth to tunnel diameter.

Then green field effects (surface settlements) and pile group settlements of tunnel excavations are studied. In this part, the settlements at the immediate i.e. tunnel advancement reaches below the center of pile group and at the plain strain condition i.e. the advancement passes the center of pile group are considered. Out puts of displacement in the soil, settlements in group pile, change of skin friction along the piles, load transfer mechanisms of group pile and differential settlements are presented and discussed.

After modeling and analyzing of the different tunnel excavation depth, out puts of displacements are presented and discussed. Conclusions are finally presented.

1.8 Structure of the Thesis

This thesis consists of five chapters. The chapters essentially reflect the order in which the research was carried out. Chapter 2 reviews previous literatures related to the research. It assess researches related on ground loss components and mechanisms, methods for predicting tunnel induced ground movement and pile deformation through empirical, analytical and numerical approaches.

Chapter 3 illustrates the study design (methodology) of the research. In this chapter, numerical methods that have been conducted to investigate the research problem are presented. Model schematics, the numerical tool (PLAXIS 3D), material parameter and tunnel advancement procedure are discussed in detail.

Chapter 4 analyses simulation results. The chapter briefly presents results related to pile load test, transverse surface settlementstrough, pile group settlements due to tunnel advancement, pile group influence zone, variation of skin friction, load transfer mechanism and differential settlements.

Conclusions drawn from this research and recommendations for future research are outlined in chapter 5.

CHAPTER TWO

2 Literature Review

2.1 Introduction

The accurate assessment of tunneling-induced effects on adjacent structures depends on the accuracy of the predicted tunneling induced ground loss values and ground deformation. At present, ground loss values are assumed based on past experience and the outcomes of previous tunneling projects under similar conditions. In reality, depending on tunneling methods, tunnel configuration, types of soil and other factors ground loss values also vary. The fact that such variation in empirical observations exists suggests the need for a more logical approach to estimating ground loss due to tunneling.

Previous researcher was developed different components of ground loss, such as face loss, shield (radial) loss and tail loss. In this study the various aspects of ground loss mechanisms are considered that covered by other researchers.

These new methods are often used before construction to predict ground loss parameters depend on known TBM geometry, geotechnical conditions and therefore the tunnel configuration. (Loganathan et al, 2005; Loganathan et al, 2000 and Loganathan and Flanagan, 2001) has proposed verified the total ground loss from case histories. Prediction of various components of ground loss presented during this monograph has not yet been verified; however, such verification is planned for the longer term. It will be supported either field measurements or/and three dimensional numerical modeling, and after it's completed, this monograph are going to be updated

2.2 Definition of Ground Loss

Ground loss is defined as the volume of soil (through face or radial and tail of the shield) that has been excavated in larger than the volume of excavation in theoretical design. In this study, ground loss estimation assumes uniform radial ground movement (average ground loss) and is denoted as VL (%). In reality, because of gravity effect the ground soil loss around the tunnel is non uniform seems like oval shape.

2.2.1 Ground Loss Components and Mechanisms

Tunnel excavation causes different ground loss by different direction. This is associated with ground movement. When the excavation time the loss occurred different direction (front, side, rear) the total value of these loss are known as ground loss or volume loss. The components are namely face loss, radial loss (shield loss) and tail loss as shown below Figure 2.

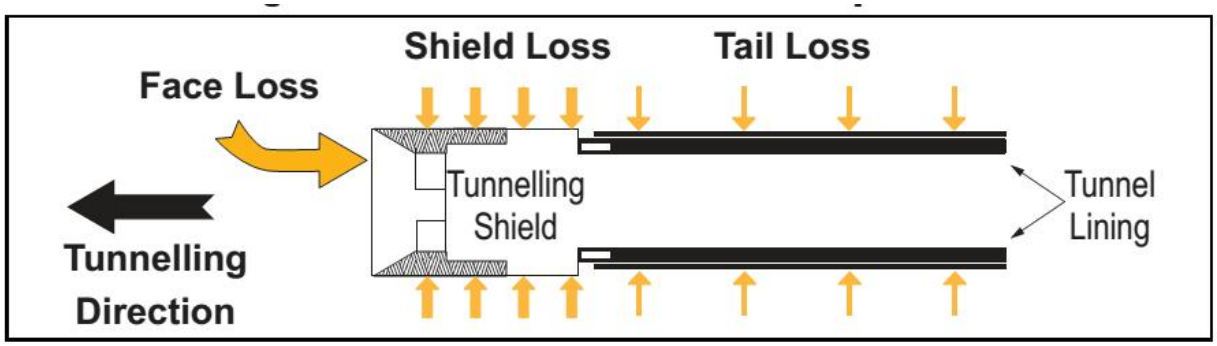

Figure 2-1 Various ground loss component (Loganathan, N., 2011)

The process of ground loss components are as follows:

• **Face loss when** the loss occurs at the front face of the TBM during excavation. That means the ground stress changes because of excavation. When change in ground stress at the face of TBM causes longitudinal ground movement into the tunnel face.

• **Shield loss** when the loss occurs radially around the TBM which is a larger diameter than the actual size of the tunnel this creates the gap between the ground and lining and reduces the soil friction of TBM.

• **Tail loss** it occurs during lining stage of the tunnel incomplete filling of the grout or pea gravel that is applied to the tail gap immediately after the segmental lining leaves the TBM shield.

2.3 Previous Research Methods for Predicting Tunneling Induced Ground Movements

To calculate the estimation value of soil movement (ground loss) due to tunneling excavations classified in to three methods; empirical, analytical and numerical. The method and the demerits of each method are discussed below.

2.3.1 Empirical Method

Surface Settlement. By using empirical data first of all first of all estimate settlement in soft ground. Most commonly used empirical calculation was proposed by Peck (1969), he investigated the shape of surface settlement represented by distribution curves, or error curves based on a number of field measurements, as shown in Equation 2.1.

$$S = S_{max}.exp\left(\frac{-X^2}{2i^2}\right) \quad (2.1)$$

Where:

S = vertical settlement of surface in the direction of x from the tunnel centre line

S_{max}= maximum surface settlement at x=0

i = point of inflexion. At the location of maximum settlement

The maximum settlement can be computed by using Equation 2.2 as proposed by Mair (1993):

$$S_{max} = \frac{0.313V_L D^2}{i} \quad (2.2)$$

Where

V_L= ground loss (ratio of ground loss volume/tunnel volume per meter length)

D = diameter of the tunnel.

Figure 2.2 shows different hypothetical prediction of surface settlement trough 6-m diameter tunnel at a 30-m depth. The ground loss ratio (ground volume/tunnel volume) was assumed as 1 %. The maximum surface settlements estimated by different methods are range of 7 mm to 10 mm. The surface settlement trough width, i, varies from 8.3 m to 15 m These results show the variability of empirical predictions proposed by various researchers due to the variability in the databases they used for the derivation of i values Loganathan, N., 2011.

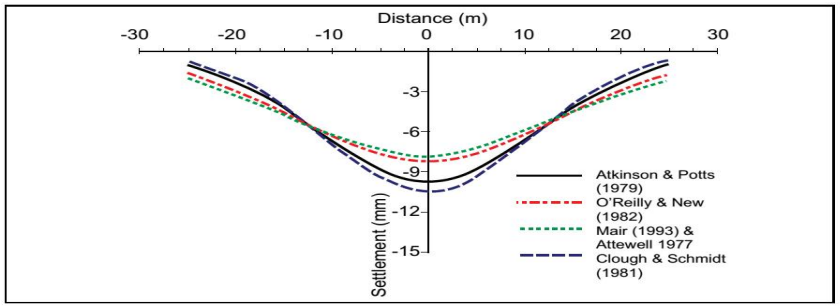

Figure 2-2 Various prediction of surface settlement trough by Loganathan, N., 2011

A significant amount of research devoted to estimate S_{max} and the i values for different ground conditions by involving field observations and model tests. The estimations of i values by various researchers are such as shown in Table 2.1.

Table 2.1 Different estimation value of i

Name	i-Value	Remark
Pech (1998)	$\frac{i}{r} = \left(\frac{z_o}{2R}\right); n = 0.8 to 1.0$	Based on field observation
Atkinson &Potts (1979)	i=0.25$(z_0 + R)$: $for loose sand$ i=0.25$(1.5z_0 + 0.5\,R)$: for dense sand And over Consolidated Clay	Based on field observation and model test
O'Reilly &New (1982)	i=0.43z_0 + 1.1: cohesive soil i=0.28z_0 + 0.1: granular soil	Based on field observation of UK tunnel
Mair (1993)	i=0.5z_0	Based on field observation worldwide and centrifugal test
Attenwell (1977)	$\frac{i}{R} = \alpha.\left(\frac{z_0}{2R}\right)$ α = 1and n=1	Based on field observation of UK tunnel
Clough &Scheldt (1981)	$\frac{i}{R} = \alpha.\left(\frac{z_0}{2R}\right)$ α = 1and n=0.8	Based on field observation of UK tunnel

Note:Z_0 is the depth of the tunnel below the ground (at tunnel springline) and R is the tunnel radius on Table 2.1

Subsurface Settlement. Now a day, the prediction of subsurface settlement profiles has empirical method of calculation. Mair (1993) and Atkinson & Potts (1979) proposed two most commonly used empirical methods.

Mair (1993) proposed that the shape of subsurface settlement profiles is similar manner as surface settlement profiles characterized by Gaussian distribution. in the same manner as for surface settlement profiles. His empirical method proposed for calculating the subsurface settlement is shown Equation 2.3:

$$S = S_{max}.\exp\left(\frac{-X^2}{2i^2}\right) \quad (2.3)$$

Where $i_z = K(Z_0 - Z)$

$$K=\frac{0.175+0.325\left(1-\frac{Z}{Z_0}\right)}{1-\frac{Z}{Z_0}}$$

Therefore:-

$$\frac{S_{z,max}}{R}=\frac{1.25V_L}{0.175+0.325\left(1-\frac{Z}{Z_0}\right)}.\frac{R}{Z_0}$$

Atkinson & Potts (1979) investigated the estimated Equation of subsurface settlement base on model test as shown below.

$$\frac{S_Z}{S_{z,max}}=1.0-\alpha\left(\frac{Z-R}{2R}\right) \quad (2.4)$$

Where:

α= 0.57 for dense sand

α = 0.40 for loose sand

α = 0.13 for over-consolidated clays

Sz = settlements at depth z

$S_{z,\ max}$ = maximum settlement at depth z.

Vermeer and Bonnier (1991) proposed a similar empirical formula:

$$s_z=\left(\frac{z_0}{z_0}\right)^2 s_{z,max} \exp\left(\frac{-x^2}{2i_z}\right) \quad (2.5)$$

Nor grove et al (1979) established an empirical relation as a ratio of the subsurface settlement;

$$s_x= \frac{X}{Z_0} S_Z \quad (2.6)$$

Where:

Sx = lateral deflection

Sz = settlement at depth z

x = lateral distance from the tunnel centre line

Z_0 = depth of the tunnel.

Limitations of empirical method:

•Do not give accurate surface settlement value

•Their applicability to different ground conditions and construction techniques

•Horizontal movement and surface settlement have limited.

2.3.2 Analytical Method

Different parameters are affecting the ground deformation prediction values of surface settlement induced by tunneling. These parameters include

• Method of construction and tunnel advancement details
• The diameter and depth of tunnel
• Ground water table condition
• The initial stress state
• The different strength behavior of the soil around the tunnel.

Current "rules" for estimating ground settlement from tunneling operations were derived generally from empirical correlations between some of those variables and the settlements observed in actual tunnels, as described in Section 2.3.1. Hence, they account for only a few

of the significant factors, and extrapolation to other cases is questionable mainly because similar conditions are generally not fulfilled. Only a few attempts to develop analytical methods (closed-form solutions) that incorporate all factors contributing to ground deformations have appeared:

• Sagaseta (1987) investigated for incompressible, isotropic soil strain fields that near to the tunnel by using closed form analytical solution.

• Verruijt and Booker (1996) also proposed the analytical solution for homogeneous elastic half space of tunnel.

Sagaseta's generalized the Verruijt and Booker solution in that it:

• determine the value of ground loss for incompressible soil and different value of Poisson's ratio.

• In long term deformation solution includes ovalisation effect

Verruijt and Booker's(1996) determination of surface settlements and lateral deformations in closed form solutions as follows:

Surface settlements**:**

$$U_Z=-\varepsilon R^2\left(\frac{Z_1+Z_2}{r_1^2+r_2^2}\right)+\delta R^2\left(\frac{z_2(kx^2+z_2^2)}{r_1^4}+z_2\left(\frac{kx^2+z_2^2}{r_2^4}\right)\right)$$

$$+\frac{2\varepsilon R^2}{m}\left(\frac{(m+1)z_2}{r_2^2}+\frac{mz(x^2-z_2^2)}{r_2^4}\right)-2\delta R^2\mathrm{h}\left(\frac{x^2-z_2^2}{r_2^4}+\frac{m}{m+1}\frac{2zz_2(3x^2-z_2^2)}{r_2^6}\right) \quad (2.7)$$

Estimation of lateral deformations:

$$U_x=-\varepsilon R^2\left(\frac{x}{r_1^2}+\frac{x}{r_2^2}\right)+\delta R^2\left(\frac{z_1(1x^2+kz_1^2)}{r_1^4}+\frac{x(x^2-kz_2^{26})}{r_2^4}\right)$$

$$-\frac{2\varepsilon R^2x}{m}\left(\frac{1}{r_2^2}-\frac{2mzz_2(x^2-z_2^2)}{r_2^4}\right)-\frac{4\delta R^2\mathrm{xh}}{m+1}\left(\frac{z_2}{r_2^4}+\frac{mz(x^2-3z_2^2)}{r_2^6}\right) \quad (2.8)$$

Where

$\varepsilon =$ uniform gradial ground loss

$\delta =$ deformation of ground due to the ovalization of the tunnel lining

$z_{1=z*H}$

$z_{2=X*H}$

$r_1^2=X^2 + Zr^2$

$r_1^2=X^2 + Zr^2$

R and h tunnel radius and water table

$m=1(1-2v)$

$m=v/(1-v)$

v = poison's ratio of soil.

2.3.3 Numerical Method

Some of the limitations in empirical methods (and, consequently, analytical methods) may be overcome by the finite element method, which indeed has been used widely for tunneling analyses. For example, Rowe and Kack (1983) found in their analyses of some case

Histories that their finite element technique generally gave good prediction of soil settlements as compared with those measured, although unfavorable comparisons were found in some cases. Successful predictions of lateral soil movements by the numerical method were also reported by Lee et al. (1992). Gunn (1993) reported that a finite element analysis gave poor predictions for surface settlements, however, even with a refined constitutive soil model. Gunn found that the surface settlement trough was too wide and shallow compared with those given by the empirical methods (error curve) and field measurements.

Simpson et al. (1996) concluded from their analyses of excavation in London Clay that the predicted surface settlement trough was substantially influenced by the anisotropic shear modulus, but that it was little influenced by non-linearity of ground stiffness. Addenbrooke (1997) reported that better predictions could be achieved by using sophisticated soil models that accounted for non-linear soil behavior at small strain.

Xiang et al. (2008) investigated the effect of tunneling in clayey and sandy soil on urban piled over pass structures of Beijing metro station. Their study involved empirical, theoretical and numerical (using Mohr-Coulomb Model) predictions and in situ monitoring data. From in situ data, they found that the post-underpinning pile foundation showed a large amount of additional settlement prior to behave like the nearby non-under pinned pile foundation, for the same tunneling influences. They concluded that the surcharge effect from an existing structure on the ground increases the effect of tunneling on ground deformation. Also they recommended that the general control procedure should consist of assessing the superstructure Capacity, prediction of tunneling and dewatering-induced ground surface and pile foundation settlements, establishment of criteria for distinctively constraining ground surface, pile foundation settlements, and execution of reinforcement measures for metro tunneling in closer to an existing urban overpass supported on pile foundations.

Vahdatirad et al. (2010) adopted this model in studying the effect of boring the tunnel of Tabriz, Iran on an underground commercial center which is located on the tunnel passage. The soil type that had been excavated is silty sand. They presented the risk level assessment for settlements of a commercial center foundation due to tunneling. Empirical and numerical methods using Mohr-coulomb model were used to obtain the value of the underground commercial center structure settlement.

The findings of various researchers appear contradictory in terms of the selection of appropriate soil models for predicting tunneling-induced ground deformations. Finite element predictions require considerable expertise, modeling and interpretation skill to obtain accurate results. Further, the following aspects need to be modeled accurately:

• The realistic stress path that soil (soil-structure interaction mechanism) experiences during the tunnel excavations for different tunneling methods

• The three-dimensional effect of various ground loss components, typically face loss and the radial ground loss

• The stress-strain behavior of the soil around the tunnel.

2.4 Pile Deformation Induced by Tunneling: Physical Observations

2.4.1 Field Observation

To investigate the impact of tunneling on piles and pile toes, Kaalberg et al. (2005) conducted a full-scale trial test at the Second Heinenoordtunnel within the Netherlands. The authors argued that tunneling had a minor impact on pile stress relief, and they constructed a tunnel influence zone based on the varied ratios of surface and pile settling. Besides,

The building of a hand-dug escalator tunnel extremely close to pile foundation was described by Mair et al. (1993) and Lee (1994). (1m clearance between tunnel and pile). The under-reamed bored piles with a diameter of 1.2m were put below the tunnel depth. Prior to tunneling, both in-ground and in-pile instrumentation were conceivable. The nearest pile was only subjected to a maximum lateral deviation of 8mm, resulting in a volume loss of up to 2%, according to the in-pile inclinometer measurements. Furthermore, the results of the in-ground and in-pile inclinometers were nearly identical. The authors concluded that in London Clay, a tunnel could be built quite near to a pile foundation with only minor horizontal deflection.

2.4.2 Case Studies

The settlements of three piled-bridge foundations, one on end bearing piles and two on friction piles, were monitored by Jacobsz et al. (2005). The expected settlement can be compared to actual conduct in these circumstances. Bored and friction piles were subjected to various mechanisms that influence pile behavior, which will be addressed in greater depth later. The authors suggested that pile capacity be re-evaluated because loads often contain a substantial factor of safety and redistribution of weight is conceivable.

2.4.3 Centrifuge Test

Within pile instrumentation was used in only a few case studies. As a result, several researchers turned to the centrifuge modeling technique, which accurately represents soil-structure interactions while simulating true Greenfield circumstances.

Loganathan et al. (2000) used a centrifuge to model two-dimensional tunneling-induced ground movement and pile responses in stiff clay. The soil movement, axial pile forces, pile settlements,

and lateral pile deformations in Greenfield were measured and compared to analytical results. The author found that when the tunnel spring line is at or near the pile base, the bending moment and lateral deflection of a pile are critical, and when the tunnel spring line is below the pile base, the axial force is critical. . Furthermore, for similar soil-pile configurations to those used in this investigation, a roughly linear connection was detected between tunneling generated maximum bending moments and ground loss values, indicating that an elastic analysis of pile behavior may be accomplished with volume loss small

Jacobsz et al. (2004) investigated the surface settlement and load distribution of a single driven pile in dense sand with varying volume losses due to tunnel excavation. All of the tests were done with the pile base elevated above the tunnel. The zone of influence for substantial pile displacements was determined. Loads transfer from the pile base to the shaft gradually as volume loss increases, and substantial settling occurs once the maximum pile shaft capacity is reached.

Marshall and Mair (2011) conducted a centrifuge test based on Jacobsz et al(2004) .'s research and looked at the impact of installing piles prior to tunnel excavation. The installation of the driven piles, according to the authors, drastically altered Greenfield displacements, implying that analytical approaches that use Greenfield displacements as an input to determine pile reactions are ineffective when dealing with driven or jacked piles. In addition, the tunnel crown and base of the pile yielded the soil displacement value. It has been demonstrated that, depending on the placement of the pile, strains generated from pile-tunnel contact could be used to combat Greenfield soil strains.

Three centrifuge tests look at tunnels that are modeled beneath or at the level of pile toes. Chiang and Lee (2007) conducted a series of centrifuge tests to explore the responses of a single pile to digging in sandy ground under varied operating loads. Pile responses were evaluated at different tunnel embedding depths, and two distinct pile load transmission techniques were proposed. The authors believe that only the depth ratio has a substantial impact on the distributions of bending moments along with the piles, although the profiles of the axial forces are determined by both the depth ratio and the working load on the pile. The authors conclude from centrifuge results that the higher the working load on the current pile prior to tunneling, the greater the settlements the pile will experience after tunneling.

Both of the aforementioned cases involve driven piles. The consequences of tunneling beneath bored piles in clay were investigated using centrifuge model experiments by Mair and Williamson (2014). A single pile above the tunnel centerline settles more than the amount of surface settlement at the pile head, according to the simulation. Even with severe tunnel volume loss, very minor load redistribution was observed, and pile failure was not observed.

2.5 Pile Deformation Induced by Tunneling: Prediction Methods

2.5.1 Empirical Approach

In practice, empirical formulas based on field data are frequently used to describe ground deformations. The transverse settling trough is predicted using Peck's normal (Gaussian) distribution curve. Nonetheless, it lacks a theoretical foundation.

Jacobsz et al. (2005) used the Greenfield displacements at the pile base as the pile head settling to simplify the problem. For pile tip displacements, such techniques are usually cautious. Furthermore, empirical methods have significant drawbacks, such as the limited information they provide about subsurface settlement and the application of varied tunnel designs, ground conditions, and building procedures..

2.5.2 Analytical Approach

Loganathan and Poulos (1998) offered an analytical method for redefining the traditional ground loss parameter in relation to the gap parameter proposed by Lee et al. (1992) and including the equivalent ground loss parameter into Verruijt and Booker's (1998) closed-form elastic solutions. Tunnel-induced surface and subsurface settlements, as well as horizontal movement in clays, may now be predicted using this new method. A retrospective analysis of five case studies was used to determine whether the proposed strategy was applicable. The anticipated settlement troughs are slightly wider than those seen in the field or approximated using empirical approaches. However, for homogenous clay profiles, good agreements for subsurface and horizontal soil movements have been demonstrated.

Chen et al. (1999) investigated the lateral and axial responses of a single pile using a two-stage methodology. Greenfield soil motions were computed in the first step using Loganathan and

Poulos' (1998) analytical approach. The estimated soil movements were then imposed on boundary element analyses to compute the pile reactions in the second stage. Parametric studies established the design charts, which were then validated by a back analysis of a case history. However, placing Greenfield displacements on piles ignores the impact of pile placement prior to tunnel excavation.

2.5.3 Numerical Approach

To investigate the effect of TBM advancement on pile foundations, Mroueh and Shahrour (2002) used three-dimensional finite element modeling. To reflect the impact of shield, over-cut, and tail void grouting, a simpler stress release zone was created. There was no back-analysis of any physical data. During the excavation process, the variations in pile reactions such as axial forces, bending moment, and deflection were shown. The findings revealed that the longitudinal impact of tunneling on piles is substantially greater than the lateral impact. Furthermore, soil movements with the presence of a pile were compared to Greenfield data, with the authors claiming that the greenfield soil movement calculation is incorrect. The finding still needs to be validated because the impact of pile placement was not highlighted, which could damage the soil around the pile. This study also discovered two separate configuration-related failure mechanisms, confirming Loganathan et al (2000) centrifuge.'s test results.

Lee and Ng (2005) investigated the influence of a progressing open face tunnel excavation on a neighboring laden pile using a three-dimensional, elasto-plastic, coupled consolidation finite element analysis. The numerical model was built using the experimental values from Loganathan et al (2000) .'s centrifuge test. The research primarily looked at the interaction between the tunnel and the pile as it moved forward, or longitudinally. One tunnel diameter forward of and one diameter beyond the excavation face was identified as a zone of influenc. The effects of pore water pressure on surface and subsurface settlement, as well as pile responses as the tunnel progressed, were depicted. The longitudinal and transverse bending moment results were compared and found to be compatible with those of Mroueh and Shahrour (2002). Furthermore, the findings of the centrifuge model and analytical predictions calculated by the specified volume loss were compared to plain strain surface and subsurface settlements, which showed comparable tendencies.

Instead of merely removing forces corresponding to initial stress states, Cheng et al. (2007) suggested a displacement-controlled method to model tunneling processes, which tends to forecast the erroneous shape of ground displacement profile, and therefore wrong forces in piles. Back analysis of a centrifuge test and a field case study confirmed the appropriateness of the DCM, which simulates tunneling by applying displacement to the tunnel boundary.

2.6 Understanding the Response of Pile

This section compares all of the published field observations and attempts to uncover some commonalities in their findings in order to better understand pile responses to tunneling. The bending moment and axial force are represented using the following sign conventions: compressive axial forces are viewed as positive and bending moments are treated as positive if they work to bend the pile away from the tunnel. It's worth noting that the piles described in the summary below are both working piles.

2.6.1 Load Distribution and Transfer Mechanism

Tunnel-pile configuration has a significant impact on pile responses, according to centrifuge testing. In actuality, two common circumstances are encountered: (a) tunneling beneath the pile tip, referred to as deep tunneling, and (b) tunneling near to or above the pile tip, referred to as shallow tunneling, both of which develop different load transfer mechanisms prior to failure.

The pile base resistance will first be reduced due to stress relief of tunneling when the tunnel is built at or below the pile tip. The base resistance is transferred to the pile shaft to achieve load equilibrium, resulting in increased positive skin friction along the pile. A greater pile settlement is expected if the additional positive skin friction cannot compensate for the unavoidable considerable loss of end bearing capacity. Furthermore, in this case, the lateral response of the pile is unlikely to be significant.

In the second situation where the tunnel is constructed above or some distance far from the pile tip, a different mechanism is observed. The stress relief due to tunneling causes negative skin friction to act along the pile shaft above the tunnel level. To maintain the equilibrium, the pile shaft below tunnel level (which can be seen as a fixed end) would support the drag-load from the upper part so that positive skin friction increases. Only when the positive shaft resistance and

pile base are fully mobilized, the settlement would become a problem. Compared to the potential pile settlement, the lateral pile response can be significant since horizontal soil movement is the biggest near the tunnel. Because horizontal soil movement is the greatest near the tunnel, the lateral pile response can be large when compared to potential pile settling.

2.6.2 Vertical Deformation of Pile

Pile settling is primarily determined by the depth ratio of the tunnel and pile, i.e. Lp/Htunnel, where Lp is the pile length and Htunnel is the tunnel axis embedded depth. The depth ratios of Lp/Htunnel 1 and Lp/Htunnel> 1 correspond to the concepts of deep tunneling and shallow tunneling in the previous section, respectively. Chung stated that significant pile settlement is only a worry when Lp/Htunnel is less than 1. When the pile tip is placed above or near the tunnel, Jacobsz et al. (2004), Kaalberg et al. (2005), and Selemetas et al. (2005) each identified their own but similar zones of influence. Later, a more detailed description of the influence zone will be provided. Depending on the position of the pile tip in zones, the ratios between pile settlement and surface settlement vary. Furthermore, Lee and Ng (2005) discovered that if the pile-tunnel clearance in the longitudinal direction is smaller than one tunnel diameter, pile settlement is significant.

Jacobsz et al. (2004) used a centrifuge model with single axial loaded piles driven in dry sand to conduct a parametric research, and similar zones of influence were found. As illustrated in Figure 2.6, the settlements of piles in various locations around the tunnel revealed an approximately parabolic-shaped zone of influence. The possibility for a substantial settlement was chosen as a criterion, which is 20 mm at prototype scale and exists at volume loss larger than 1.5 percent. Within the zone, it was further split by numerous lines based on pile settling at a volume loss of 1.5 percent when compared to surface settlement.

2.6.3 Axial Load of Pile

Chiang and Lee (2007) discussed load transfer procedures for shallow tunneling (Lp/Htunnel> 1) and deep tunneling (Lp/Htunnel 1). When Lp/Htunnel> 1 and Lp/Htunnel 1, the author observed that pile axial force is greatest at the tunnel spring line level and lowest at the pile head level. Loganathan et al (2000) centrifuge .'s test findings support this trend.

2.6.4 Bending Moment of Pile

Because the bottom portions of the pile act like a fixed end, Chiang and Lee (2007) discovered that piles with pile tips far below the tunnel horizontal axis have both positive and negative bending moments for the top and lower portions of the pile, respectively. A negative bending moment developed along the entire length of the pile in the case of Lp/Htunnel 1. In this circumstance, the bottom regions of the pile behave like a free end.

Due to the simulation of a plane strain tunnel, the majority of investigations have focused on transverse bending moment. Mroueh and Shahrour (2002) used a computer simulation to show that the transverse bending moment is roughly three times greater than the longitudinal bending moment in a three-dimensional tunnel. Lee and Ng (2005) both agreed with this conclusion.

2.7 Zone of Influence of Pile

In engineering practice, the influence zone is commonly utilized as a guideline to control tunnel location in relation to nearby pile foundations. Several studies have developed specific effect zones based on a variety of factors, such as typical shear surface, pile settlement, normalized pile head settlement, and building settlement. These criteria are summarized and assessed in the following sections.

2.7.1 Shear Plane

Figure 1 depicts the influence zone, which is defined by a line with an angle of = 45°′/2 to the vertical, where ′ is the soil's effective friction angle. This line, which runs from the tunnel boundary to the ground surface, is based on the typical shear surface proposed by Morton and King (1979) based on model test results. The shear surface was then connected to the ground with a wedge of width 2.5 starting from the tunnel lining proposed by Attewell et al. (1986), where is the distance between the tunnel central line and the point of inflection.

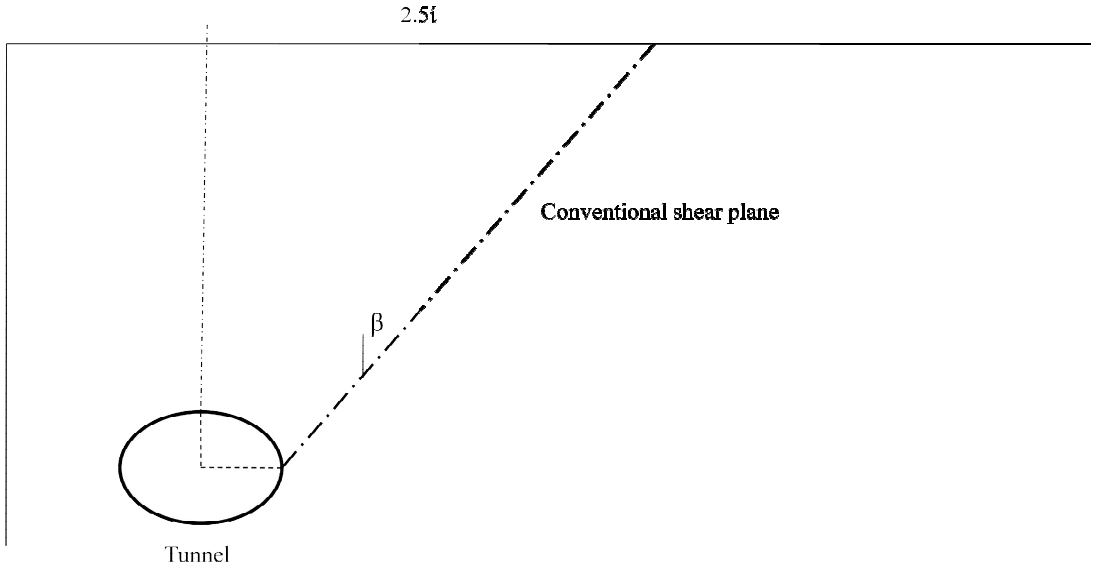

Figure 2-3 Shear plane influence zone

2.7.2 Settlement of Pile Head

According to Kaalberg et al. (2005), piles near the tunnel can be divided into three categories, as shown in Figure 2.4. The settlement of piles located in Zone A is greater than surface settlement. When the settlement is in Zone B, it is virtually identical to surface settlement, and when it is in Zone C, it is nearly identical to pile settlement

Selemetas et al. (2005) conducted a full-scale trial during the construction of the new Channel Tunnel Rail Link (CTRL) in the UK and identified three zones of influence in which pile head settlements were correlated to surface ground settlements, according to Kaalberg et al (2005).

R is defined as the ratio of pile head settlement to surface ground settlement, as shown in Figure 2.5. Selemetas et al. (2005) provided a more detailed description of the pile settlements in the zone when compared to the findings of Kaalberg et al. (2005). In Zone A, the ground surface was 2-4 mm higher than the piles. Zone B pilings settled at the same rate as the ground surface, while Zone C pilings settled at a slower rate.

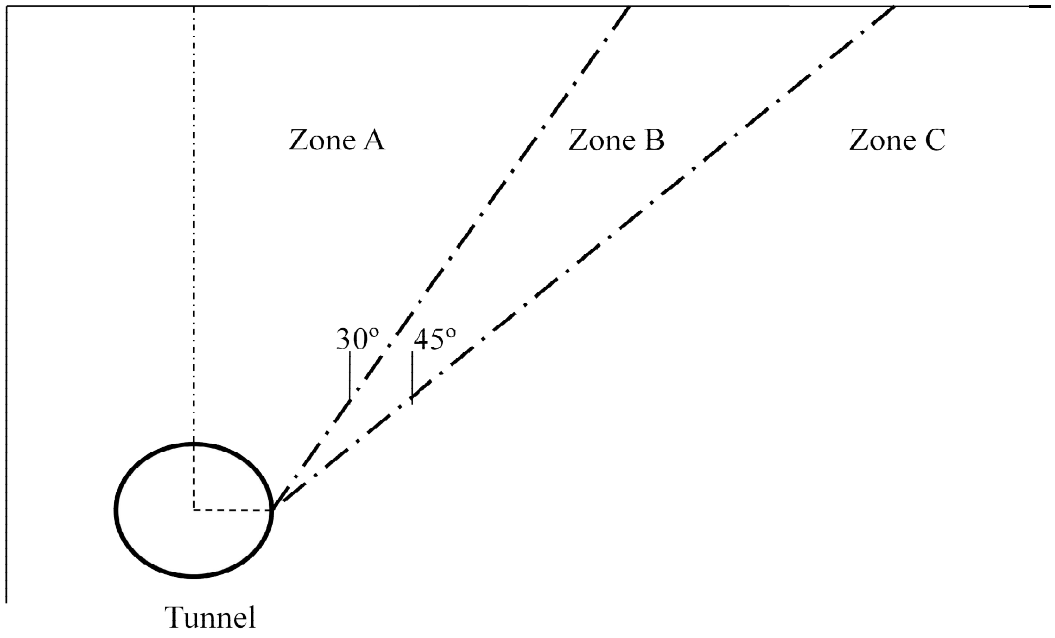

Figure 2-4 settlement zone of pile based on field observation proposed by Kaalberg et al. (2005)

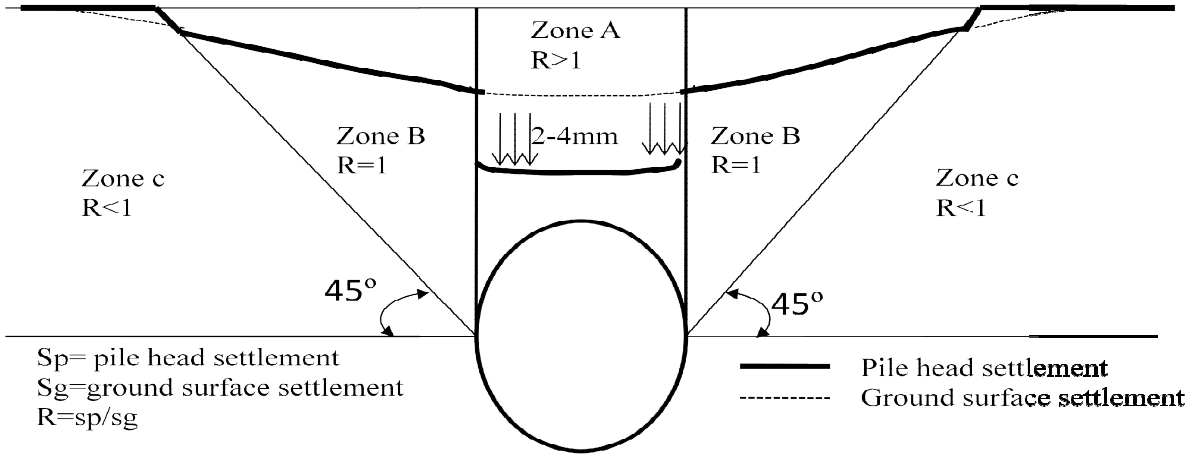

Figure 2-5 Settlement zone of pile based on field trial proposed by Selemetas et al. (2005)

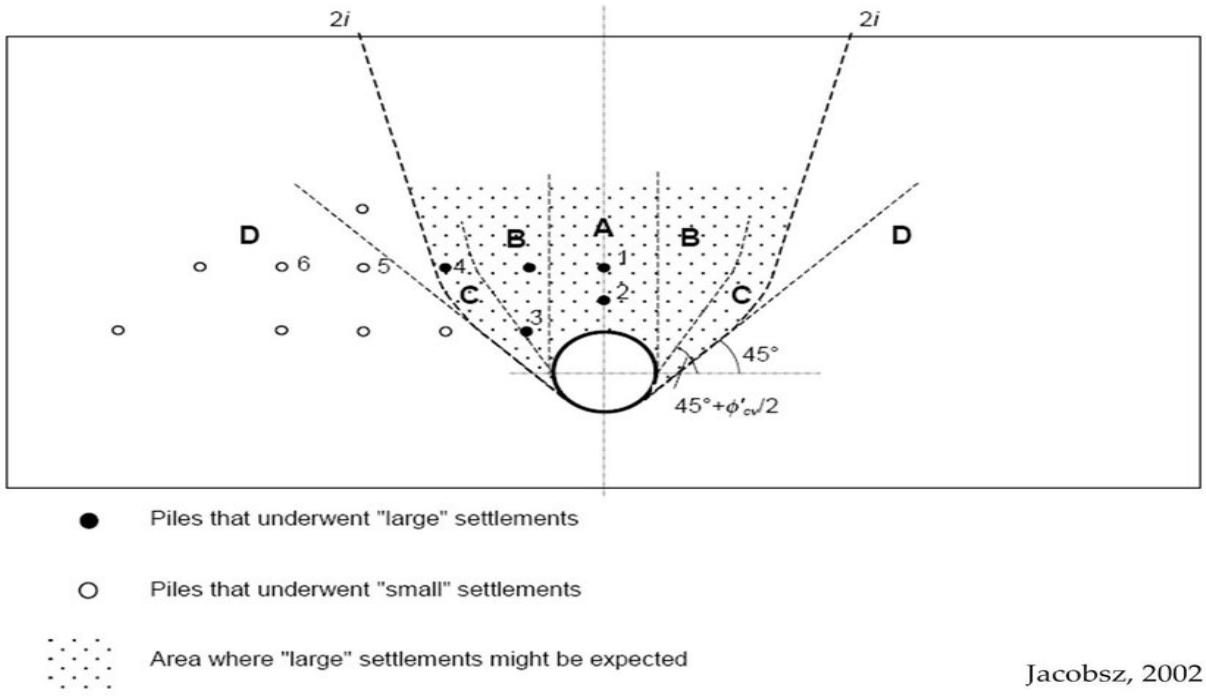

Figure 2-6 Settlement zone of pile based on centrifuge test proposed by Jacobsz et al. (2004)

2.6.4 Allowable Settlements for Structures

Unlike Jacobsz et al. (2004), Vu et al. (2015) defined the influence zone due to tunneling in terms of allowable settlement u_{max}, as well as a maximum settlement for buildings on the ground surface. Figure 2.7 shows the comparison of our findings with those of Kaalberg et al. (2005). According to Kaalberg et al. (2005), the zone with u_{max} /VL 0.4m corresponds to Zone A, while the zone with 0.04m u_{max} /VL0.4m overlaps Zone B.

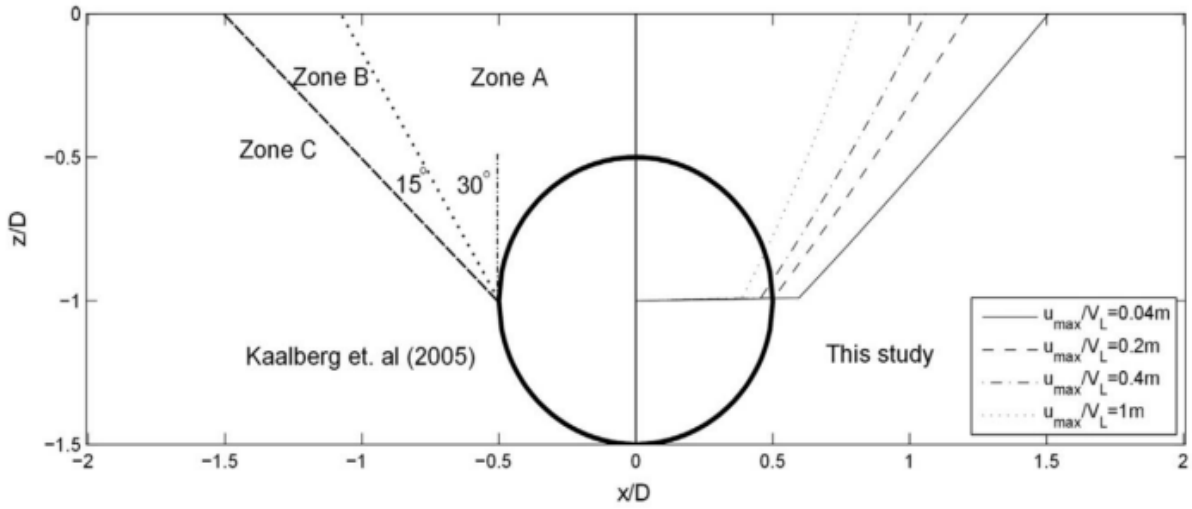

Figure 2-7 Settlement zone of pile proposed by Vu et al. (2015)

From the above literature, most of the studies have been focusing the response of pile due to tunneling on settlement, bending moment, and lateral deflection of pile. But in this study the skin friction, load transfer mechanism and differential settlement of pile group are considered.

Mroueh and Shahrour (2002) illustrated the pile response on axial force, bending moment, and lateral deflection but it has not considered the other responses.

Lee and Ng (2005) also identify zone of influence and change surface and subsurface settlements on single loaded pile, however not indicate this on group piles.

CHAPTER THREE

3 Materials Methods and Procedures

3. 1 Model Schematics

To achieve the desired objective of the study, a three dimensional finite element numerical method is employed. Selecting appropriate modeling software is a crucial step in numerical simulation. The software we choose shall provide accuracy, ease use and flexibility. In this sense PLAXIS 3D is an efficient modeling tool from the available finite element software. Hence PLAXIS is used for modeling, analysis and validation of the study. The model of the tunnel, pile foundation, and soil mass is shown in (Figure 3 .1) .The size of the model is 60 m x 80 m x 40 m (length x width x height). Group of (3 × 3) piles with spacing of s = 3 times the diameter of pile (Bowles, 1997) were modeled to investigate the behavior of the group piles, where D is the diameter of the tunnel and d is the diameter of the pile . The model dimension in the x-direction is 60 m (10 D), y-direction is 80 m (13.3 D), and in the z-direction is 40 m (6.6 D). The mesh consists of nearly 22,000 elements (10-node tetrahedrons) with over 31,306 nodes.

A fine mesh was used near the tunnel and pile locations due to the concentration of large shear strains; while a coarser mesh was used outside these zones. A constant diameter (D=6m) of tunnel is used for all analysis. As shown in Figure 3.2 the vertical profile view of the model geometry used in the group pile analysis, where E is the horizontal distance from the pile group center to center line of tunnel and C is the vertical distance between the tunnel crown and pile base. The diameter of pile and length of pile was 0.8m and 18m, respectively. The pile group and the pile cap were assuming a hinge connection, and the pile cap thickness is 1 m. In this study, the behavior of three consecutive piles of pile group was analyzed and interpreted. Figure 3.3 shows detail dimensions of pile cap and Figure 3.2 shows the pile group positions. The tunnel construction is assuming by tunnel boring machine (TBM) advancement (Chapman, 2010). The depth of ground water was assumed 2m blow the ground and the hydrostatic pore pressure was kept constant during the tunnel boring advancement. Using the principle of symmetry, taking only the half section of the tunnel is modeled.

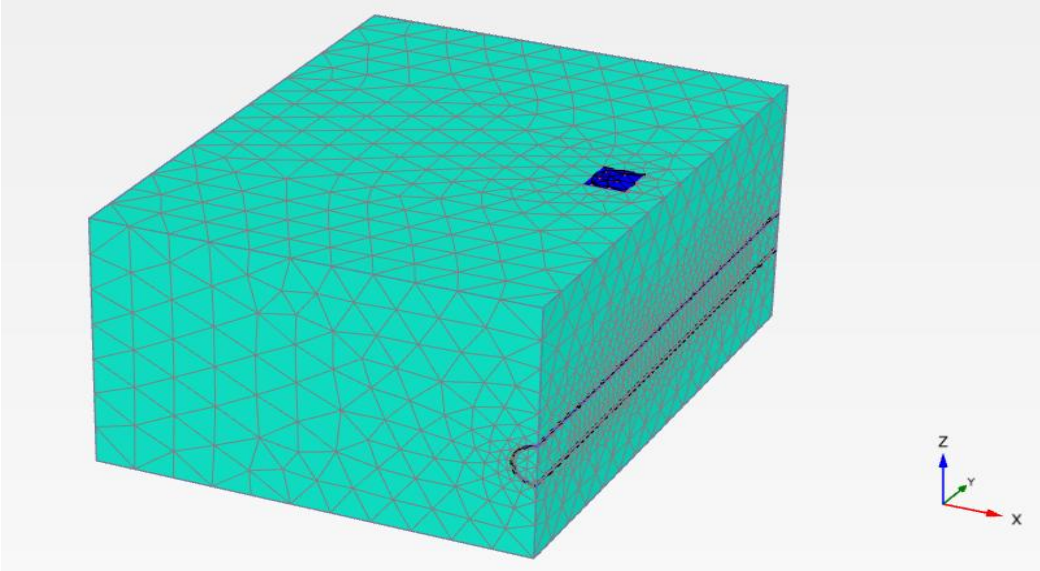

Figure 3-1 3D view of modeling mesh

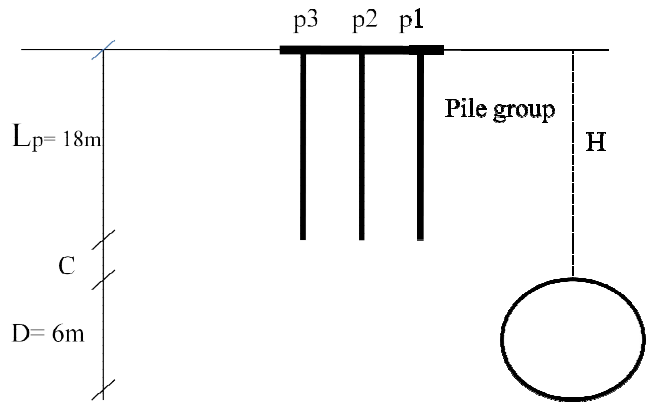

Figure 3-2 Section view of the model

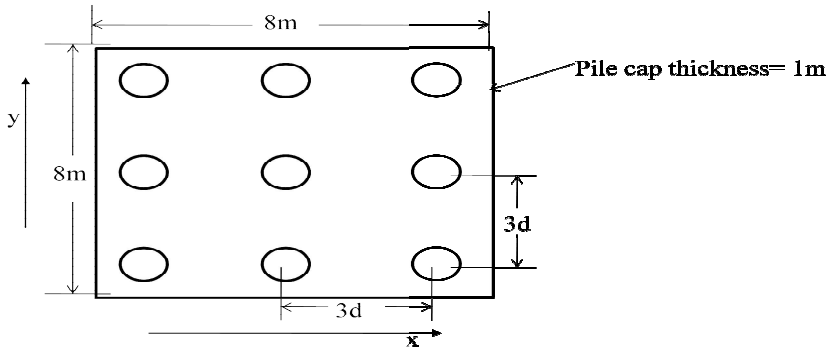

Figure 3-3 Detail dimensions of pile cap

3.2 Soil Parameters and Constitutive Soil Models

An elasto-plastic analysis was adopted to simulate tunnel construction. Pile–soil interaction was included using the embedded pile feature (Brinkgreve et al., 2013). Piles used for the model was embedded pile which is contain abeam elements that can be located any directions of soil and interact by a special interface elements.

Table 3.1 suggested reduction factor, R_{inter} (brinkgreve and shen, 2011

Interaction sand/steel	$= R_{inter} \approx 0.6 - 0.7$
Interaction clay/steel	$= R_{inter} \approx 0.5$
Interaction sand/concrete	$= R_{inter} \approx 1.0 - 0.8$
Interaction clay/concrete	$= R_{inter} \approx 1.0 - 0.7$
Interaction soil/ geogrid (grouted body) (interface is not necessary)	$= R_{inter} \approx 1.0$

Table 3.3 parameters of concrete element that used for this research. Tunnel-soil interactions were included using interface elements around the tunnel. Hardening Soil (HS) constitutive model was used for soil and isotropic elastic model was used for structures. As Zarev (2016) proposed to get a realistic estimation of deformation during the tunneling shield prefer use advanced soil model like HS and HS small Table 3.2 shows parameters of soil used for this research adopted from Miro et al., 2012.

Table 3.2 Soil parameters adopted in numerical analysis (from miro et al. 2012)

Soil parameters HS model		
Parameters	value	units
Friction angle, ϕ	35	[º]
Dilatancy angle, ψ	5	[º]
Cohesion, C	10	kN/m^2
Secant stiffness in the standard drained triaxial test, E_{ref}^{50}	35000	kN/m^2
Tangent stiffness for primary oedometer loading, E_{ref}^{oed}	35000	kN/m^2
Unloading and reloading stiffness, E_{ref}^{ur}	100000	kN/m^2
Reference pressure, P_{ref}	100	kN/m^2
Power stiffness, m	0.7	-
Failure ratio, R_f	0.9	-
Poisson's ratio for unloading-reloading, V_{ur}	0.2	-

Soil weight above phreatic level, γ_{unsat}	17	kN/m^3
Soil weight below phreatic level, γ_{sat}	20	kN/m^3
Strength reduction factor for interface in PLAXIS, R_{inter}	0.6	-

3.3 Structure Parameters

3.3.1 Embedded Pile

Different structure parameters used for analysis are listed below in Table 3.2:

Table 1.3 Concrete parameters adopted in the numerical analysis (from Al-Omari et al 2019)

Parameters	**Values**				**Units**	**Model**
	pile	Pile cap	Tunnel lining	TBM shield		
Diameter(D)	0.8	-	-	-	m	Linear elastic
Thickness(t)	-	1	0.25	0.35	m	
Elastic modulus(E)	$10*10^6$	$30*10^6$	$30*10^6$	$210*10^6$	kN/m^2	
Unit weight(γ)	25	25	25	120	kN/m^3	
Passion's ratio(V)	0.2	0.2	0.2	0.3	-	

3.3.2 Pile Skin Resistance

In this thesis pile were modeled by embedded piles in PLAXIS to simulate the interaction of pile with the neighboring soil. The skin and base resistance of pile are an input parameter used for in PLXIS and it is important to the pile behavior run correctly.

The skin resistance at the top and bottom of the pile are soil layer dependent or homogenous (linear) options. The formulas to calculate the top and bottom of skin friction part as follow Equation 3.5.

$$F_{skin} = \pi D L_{pile}\left(T_{skin,start} + T_{skin,end}\right) \quad (3.5)$$

Where L_{pile} is the pile length. $T_{skin,start}$ and $T_{skin,end}$, skin friction at the head and the base of the pile group, respectively

When the soil is layered soil, use layer dependent calculation of skin friction depends on strength parameter and interface of the soil. As shows the following Equations:

$$T_{skin} = (c_i + \sigma_n' \tan\varphi_i) * A_s \quad (3.6)$$

$$c_i = R_{inter} C_{soil}$$

$$\sigma'_n = K_0 \sigma'_v$$

$$\tan \varphi_i = R_{inter} \tan \varphi_{soil}$$

$$A_s = \pi \mathrm{DL_P}$$

Where T_{skin} is shaft friction. C_i and ϕ_i are the strength parameters of soil. Interface reduction factor R_{inter}. A_s *is* area of shaft surface, σ'_n is the horizontal effective stress of the soil. Lp is length of pile, K_o is the lateral earth pressure coefficient at constant and σ_v is stress at vertical.

All this input parameters are calculated by hand and used as input value for PLAXIS software.

3.3.3 Pile Tip Capacity

Pile capacity divided into to one is skin resistance the other is pile tip resistance. The pile tip resistance of pile capacity is determined as follow in Equation (3.7)

$$F_{base} = \pi R^2 (C N_C + \sigma'_V N_q + \frac{1}{2} \gamma D N_\gamma) \quad (3.7)$$

Where R is the pile radius, N_q , $N_C, and\ N_\gamma$ are bearing capacity factors, D is pile diameter and σ'_V is soil vertical stress

3.4 Tunnel Advancement Simulation Procedures

The movement of tunnel advancement process of the TBM and the late installation of the lining at the tunnel periphery cause soil stress relief around the tunnel. for this reason, radial and longitudinal deformations will take place in the soil body that tends to move towards the tunnel's cavity. This is commonly defined as (volume loss). Type of ground loss occurred when the TBM excavate as follow.

– face loss (ground movement occurred at the TBM face)
– shield loss (ground movement occurred at the radial part of the TBM)
– tail loss (occurred at the lining phase)

3.4.1 Tunnel Boring Machine

It is excavation machine of the tunnel. The shape of this machine is conical used for PLAXIS 3D of the model analysis. And also the ground loss occurs at this part and grout part of the tunnel so add the volume loss ratio in the part as surface contraction. The size of this machine is 9m length and 3m radius. The conical shape has 7.5m and the other is uniform circular at the rear part.

3.4.2 Front Excavation

During excavation time, the face of the tunnel has stress relief and the soil will be collapse. To stable this failure add the face pressure in front of the tunnel face to support the soil. These pressures are not uniform throughout the depth. Because active and passive pressure of the soil. So, the minimum pressure at the top and maximum pressure at the bottom of excavation is add increase linearly with depth.

Top Pressure

At the top front pressure of the tunnel if determined by Equation (3.8) act as active pressure.

$$\sigma'_{h,tot,ref,min}=\gamma' \times K_a \times h_{crown} + \gamma_w \times h_{crown} + I_r \quad (3.8)$$

$$\Delta\sigma'_{h,tot,ref,min}=\gamma' \times K_a \times \gamma_w \quad (3.9)$$

$$K_a=\frac{1-\sin\emptyset'}{1+\sin\emptyset'} \quad (3.10)$$

Where γ' is effective soil unit weight; h_{crown} is tunnel excavation height; $\Delta\boldsymbol{\sigma'_{h,tot,ref,min}}$ in Equation 3.9 is the incremental earth pressure; K_a is active earth pressure coefficient; ϕ' is friction angle of soil

Bottom Pressure

The bottom front depth of tunnel excavation determined by the following Equations. which is act as passive pressure of the soil.

$$\sigma'_{h,tot,ref,max} = \gamma' \times K_p \times h_{crown} + \gamma_w \times h_{crown} + I_r \quad (3.11)$$

$$\Delta\sigma'_{h,tot,ref,max}=\gamma' \times K_p \times \gamma_w \quad (3.12)$$

$$K_p = \frac{1+\sin \emptyset'}{1-\sin \emptyset'} \quad (3.13)$$

Where the K_p is the passive earth pressure coefficient.

Grout Pressure

Grout pressure is a pressure added in the rear part of the TBM. Which is before contraction of lining to support the soil collapse, and it is linearly increase throughout depth. The calculation as follows.

$$\sigma'_{ref} = u + \gamma' . h_{cen} \quad (3.14)$$

$$\sigma'_{inc} = u + k_0 . \gamma' . h_{cen} \quad (3.15)$$

$$k_0 = 1 - \sin \emptyset' \quad (3.16)$$

Where σ'_{ref} in the Equation 3.14 is grout pressure; σ'_{inc} in Equation 3.15 is grout pressure increasing throughout depth; u is pore water pressure at the center line; h_{cen} is length of tunnel excavation from ground to cover of tunnel; k_0 is pressure at rest coefficient.

Ground Loss

Grounds are mainly deformed on the grout portion and conical shape part machine during tunnel excavation. The equation as follows.

$$r = \frac{q_L}{q_O} \times 100\% \quad (3.17)$$

Before tunnel excavation the soil near to the tunnel was compressed because the pile installed firstly. The volume loss depends on grout pressure of the tunnel and different arengement, location and position of pile and tunnel. And also soil types are affecting ground deformation.

$$\varepsilon = \frac{OD^2_{shieldf} - OD^2_{pipe}}{OD^2_{sheild}} \times 100\% \quad (3.18)$$

Lining

Lining is constructing after the TBM pushing forward and the rear excavation part of the tunnel then after contracted the jack force is added with the thickness of the lining to push the TBM forward the formula was derived as follow according to proposed Krause (1987).

$$p_v=\beta.D^2 \quad (3.19)$$

Where is p_v jack force;$\beta$is an empirical factor constant

D is the diameter of tunnel

3.5 Meshing

Meshing is crucial step in finite element analysis, since the meshing algorithm effects the computational cost and accuracy of the analysis result .Finer mesh increase the accuracy of the result on the other hand finer mesh will have high computational cost .Hence the balance b/n computational cost and accuracy must be maintained. To achieve the balance in modeling researchers employ axis symmetry. Axis symmetry significantly decreases the domain and can use finer mesh while maintaining the problem definition and computational cost. As a result in this study a plane of symmetry is selected and half of the domain is modeled. In meshing generation a coarseness factor of 0.125 is used from literature .The meshes near the pile and the tunnel were refined with a factor of 0.625 since at this place interaction is taken place.

3.6 Construction Stage

In the phase excavation process two major assumption has been made .First to simulate the lubrication phase ,1.5 m extension were made for the unsupported span behind the tunnel boring machine .Second Since majority of volume loss occurred during the grouting phase ,the grout pressure is sated less than the overburden pressure to allow the contraction in this phase.The excavation process follow the following steps:

1. K_o Procedure

The first phase entails employing the k_o method to generate initial stress. For the initial phase, PLAXIS 3D's default parameters are used

2. Embedded Pile

Embedded pile was first used in soil mass .The pile installation procedure and induced surrounding soil movement cannot be perfectly modeled in PLAXIS 3D.For the sake of simplicity, the case of the bored pile was first considered. The default method for modeling the bored pile in PLAXIS 3D is valid, in which the soil cluster is deactivated and then the embedded pile is activated. In spite of the fact that the compression of adjoining soil due to the establishment of the pile is disregarded in this strategy, it is still satisfactory considering the moderately little unsettling influence of bored pile in reality. After the pile actuated, the vertical working load was included to the pile head all through of the excavation

3. Positioning Tunnel Boring Machine

At this stage at first in response to the applied working load, excess pore pressure need to be allowed to dissipate. Then the tunnel boring machine positioned at 30 m from the center of group pile .then tunnel excavation will be started and the surrounded soil cluster were disabled.

4. Boring Process

Now that the tunnel boring machine is placed at 30 m before the center of pile group, the tunnel boring process can be initiated. Initial excavation of 1.5 m width of soil mass is performed simultaneously with grouting then concrete lining is followed. The process is repeated until the tunnel reach 30 m behind the center of pile group.

The construction of the shield tunnel lining consists of connecting a series of concrete ring segments, of about 1.5 m long for each segment, within the TBM to form the tunnel lining and the TBM stopped to move during the lining erection. After erecting a tunnel lining ring, the boring is continued to ensure enough space to erect the next lining ring. This process is repeated until the tunnel reaches its specified location.

The lining is modeled as a linear elastic volume element and the TBM is modeled as a linear elastic plate element. The diameter of TBM is larger than the erected concrete lining hich is filled by grouting during advancement the grouting process is important to lead the settlement of the soil surface to be within acceptable limits and provides stability for the surrounding soil.

The excavation process at each segment (1.5 m) of boring is modeled as follows:

- ✓ The TBM starts to excavate the soil (deactivation of the soil finite elements at the tunnel head)
- ✓ Support the tunnel front face by applying face pressure to maintain soil collapse
- ✓ Activate the TBM shield, that is, material set that assign of the TBM plate elements
- ✓ Applying a back-fill grouting pressure to the back of the TBM to control stress relief and soil collapse after excavation
- ✓ Installing (activating) a new concrete lining ring
- ✓ repeating this step until it reaches a specific location

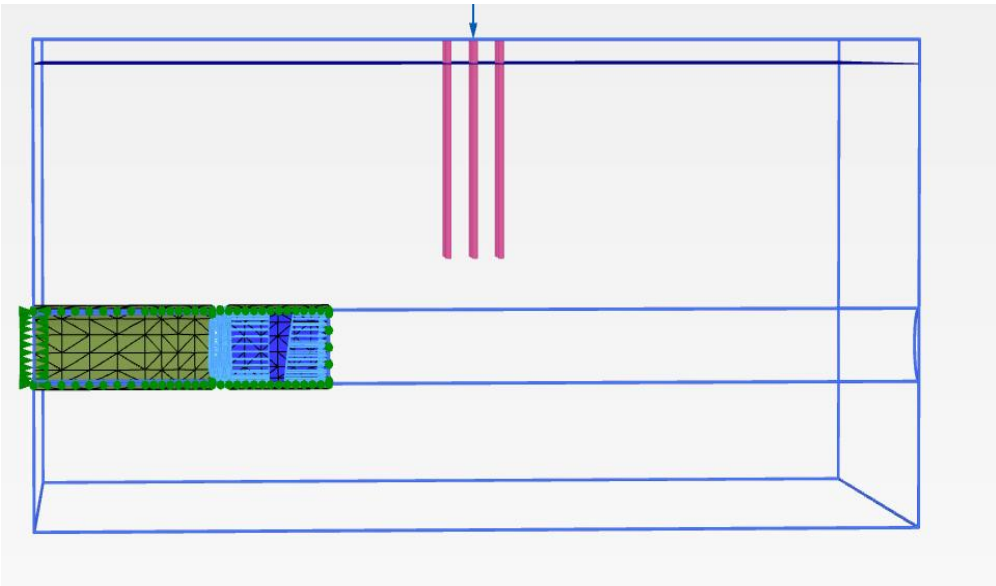

Figure 3-5 Tunnel advancement

CHAPTER FOUR

4 Result and Discussion

A series of 3D models representing a different position of tunnel excavation and group pile foundation was firstly modeled finite element software (PLAXIS 3D). Different pile deformation, skin friction reduction and load transfer mechanisms, differential settlement of group pile, and surface settlement were figured out and can be elaborated on below. Before these, the ultimate bearing capacity pile was firstly conducted in PLAXIS 3D to get the working load of the pile.

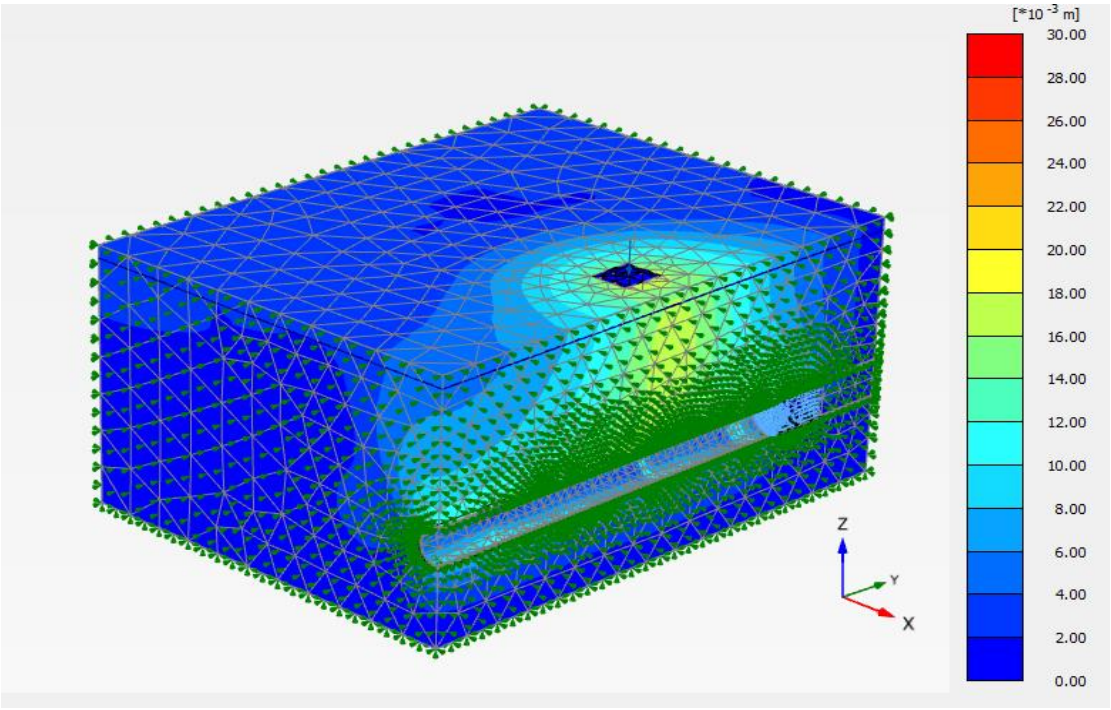

Figure 4-1 Deformation in shadings

4.1 Pile Load Test

Prior to modeling tunnel advancement, investigating the behavior of the pile group under specific geotechnical condition is vital. To calibrate the pile load test, applied load was increased from 0 to 40000kN then using equation 4.1 as suggested by Ng et al**.** 2001, the ultimate pile load capacity is determine .Figure 4.1 shows the pile load settlement curve

$$\delta_{ph,max} \cong 0.045 d_p + \frac{1}{2}\frac{P_a L_p}{A_p E_p} \qquad 4.1$$

Where; Pa = axial load,

Lp= length of pile,

Ep= modules of elasticity of pile,

Ap= pile section area

dp = diameter of pile.

As shown in Figure 4.2, the maximum load capacity of the pile group was obtained to be 18600 kN and the factor of safety is 3.0 hence dividing the maximum load with the factor of safety the service load will be 6200kN. This load is applied as axial load on the pile cap. During the working load of the pile initial pile cap settlement was calculated 7.7 mm (0.96% dp).

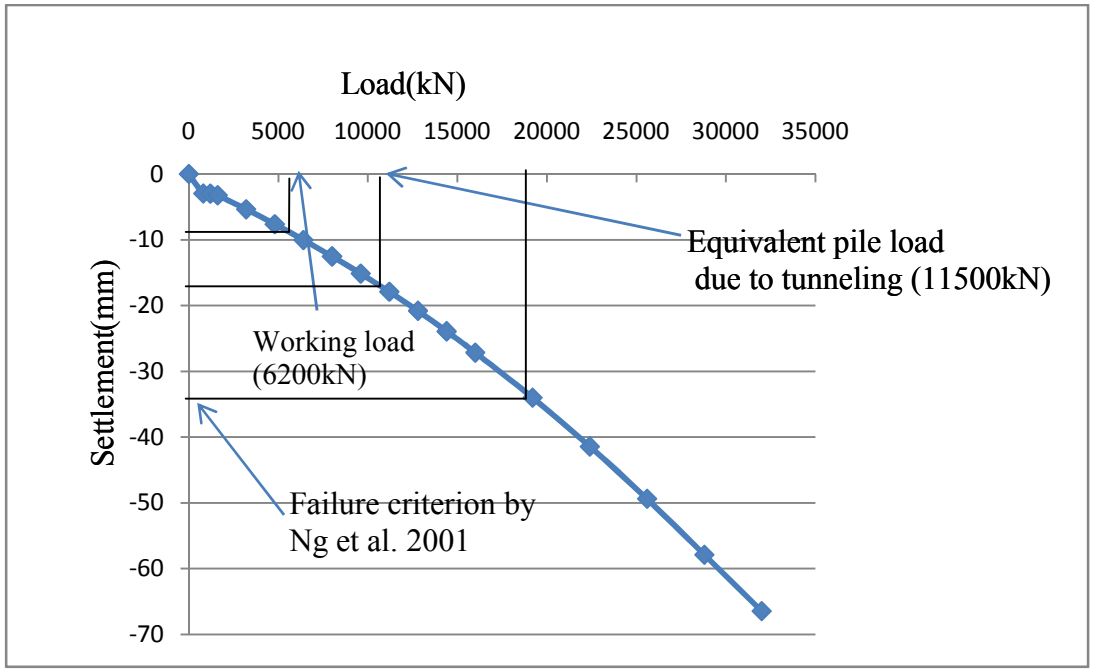

Figure 4-2 Load settlement curve of pile group from a numerical simulated pile load test

4.2 Transverse Surface Settlement Trough

Figure 4.3 depicts the normalized immediate surface settlements (S) when the tunnel face reached the monitoring section (y/D=0), while Figure 4.4 depicts the normalized plane strain condition when the tunnel face passed beyond the monitoring section at a distance of y/D≥3, for all three tunnel excavations. Although the surface settlements were considered only tunneling induces surface settlement which means the settlements obtained because of the working load are not consider. The plane strain condition of surface settlement is larger than that of immediate surface settlement. Because when the tunnel faced has passed through the monitoring section the dissipation of excess pore water pressure occurs.

At plain strain conditions, surface settlement curves are fitted with Gaussian distribution curves. Gaussian distribution curves are get from S_{max} and i (distance from tunnel centerline to the curve inflection point) that are calculated from each numerical simulation. The computed value of i at plane strain condition, are 10.66 m, 10.69 m, and 10.7 m from the tunnel centerline for H/D = 2.0, 2.5, and 3.0, respectively. The computed maximum surface settlements at the tunnel centerline are 14.17 mm, 14.49 mm and 15.02 mm for H/D=2.0, 2.5, and 3.0 respectively. Based on S_{max} and i it can be depicted that the increase of ratio H/D=3 results extreme settlement due to the pile group effect.

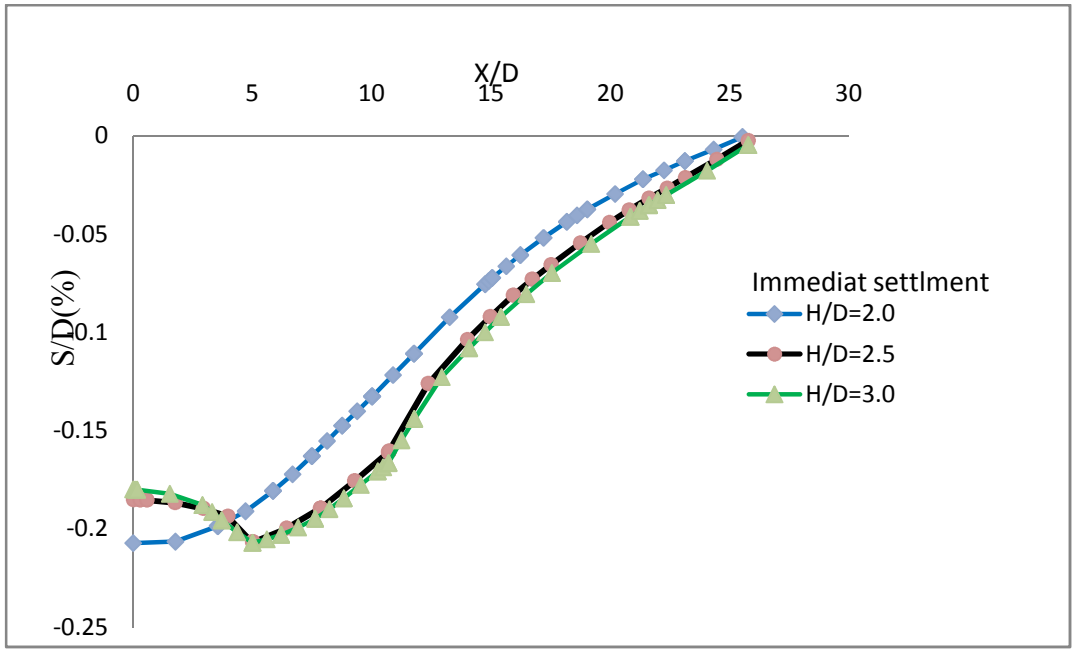

Figure 4-3Immediate surface settlement trough

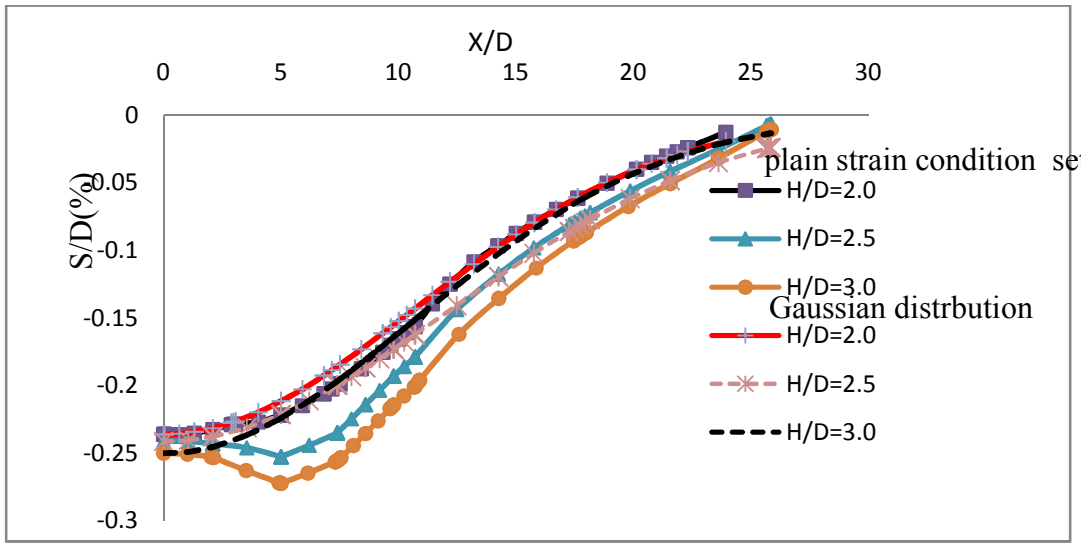

Figure 4-4 Transverse settlement at monitoring section due to tunneling

4.3 Pile Group Settlement due to Tunnel Advancement

Figure 4.5 shows the incremental settlement of pile group due to tunneling for H/D=2.0, 2.5 and 3.0.Excessive settlement in the pile group can be seen as the tunnel propels to the monitoring section.

The pile group Settlement as result of tunneling at plane strain condition (i.e. y/D≥3) at h/d =3.0, 2.5, 2.0 is 8.6mm, 7.3mm and 5.3mm respectively. It can be depicted that the settlement increase with the ratios .The total pile group settlement is 13.281mm,15.05mm and 16.33 mm for h/d 2.0,2.5and 3.0 respectively . In other word the total settlement is 1.65% dp,1.88%dp and 2.09dp for the respective ratios .It can be concluded that , in terms of percentage with dp the settlement is not much significant .The load corresponding to the biggest total settlement Which is 16.33 mm is 11500 kn , This lessens the factor of safety from 3.0 to 1.62

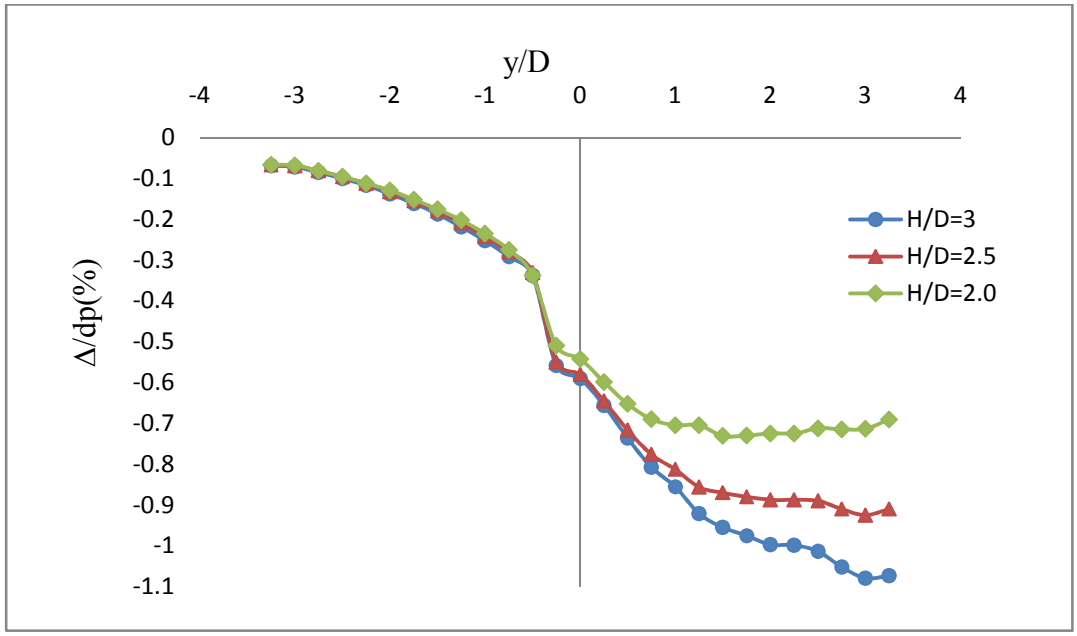

Figure 4-1 Pile cap settlement due to tunnel advancement

4.4 Influence Zone of Pile Group

From Figure 4.5 it can observe that large share of group pile settlement occurred between the rang 2D to +2D almost 80% of the settlement observe with this range. There for to decrease the settlement due to tunneling the tunnel advancement must be far from this range. That means the zone involves:

1. ± 2D from the pile in the longitudinal and lateral direction.
2. 2D vertically below the pile tip.

4.5 Pile Responses Induced by Tunneling

The behaviors of piles are divided in to two, which are the load transfer mechanism and reduction of shaft friction. The changes of the changes of pile axial load and skin friction is depicted in figure 4.6

4.5.1 The Variation of Skin Friction.

Figure 4.6, 4.7, 4.8 depicts shaft friction variation along the length of pile under different tunnel condition, respectively. When tunnel face is reach at center of pile (i.e. y/D=0).

In the case of H/D=2.0, The shaft friction reduces significantly in P1 at the upper part of the shaft (i.e.0≤z≤15), it observed that the skin friction reduced by stress relief round the shaft of P1 due to tunneling .The maximum reduced skin friction of P1 76 kPa is observed at the pile length of 12m .However, the shaft friction increases along the lower shaft part of P1 (z ≥15). And also base load of P1 is increased. Whereas the reduction shaft resistance of the pile p2 and p3 are negligible.

When the tunnel is located at C/D=2.5, shaft friction increases along the upper part of the shaft (i.e. z ≤ 12) of P1, decrease along the shaft from 12m to 15m and also increase the lower part of the shaft below 15m. Whereas negligible reduction of skin friction along the p2 and p3.

In the case of C/D=3.0, it can be showed that the skin friction increases along the upper part of p1 (z ≤12m). However the friction reduced significantly.38kPanwase reduced at the lower part of p1.there is insignificance change of skin friction along the p1 and p3.

Generally the skin friction reduces significantly when the pile near to the tunnel than far apart as it shows from p1, p2 and p3.

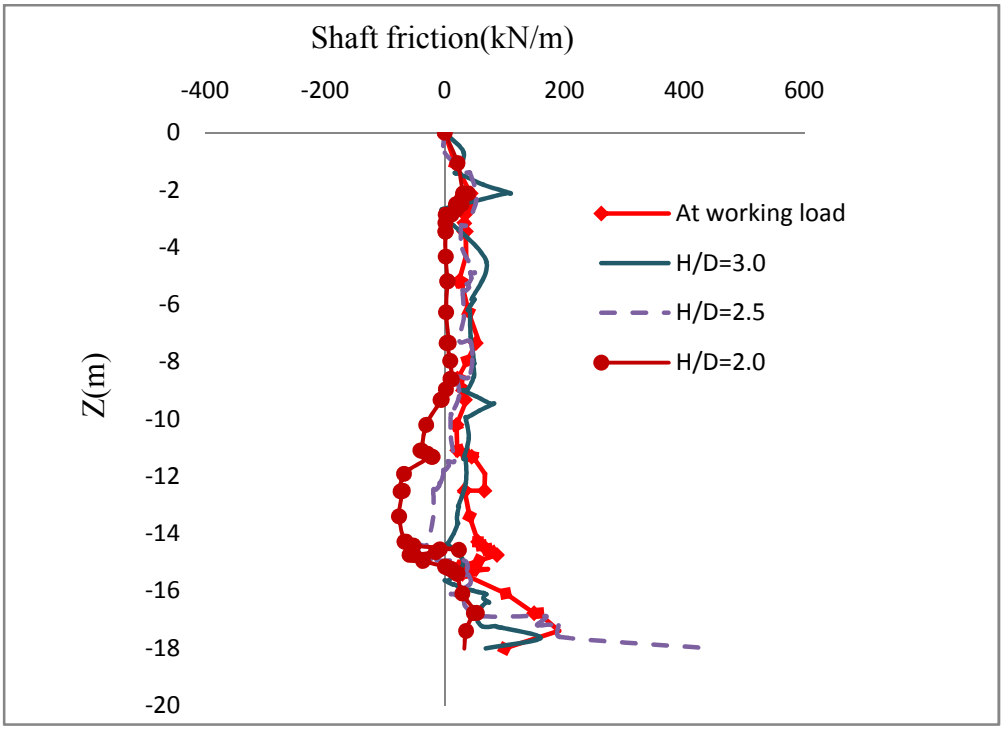

Figure 4-2 Variation of skin friction along the shaft of pile P1

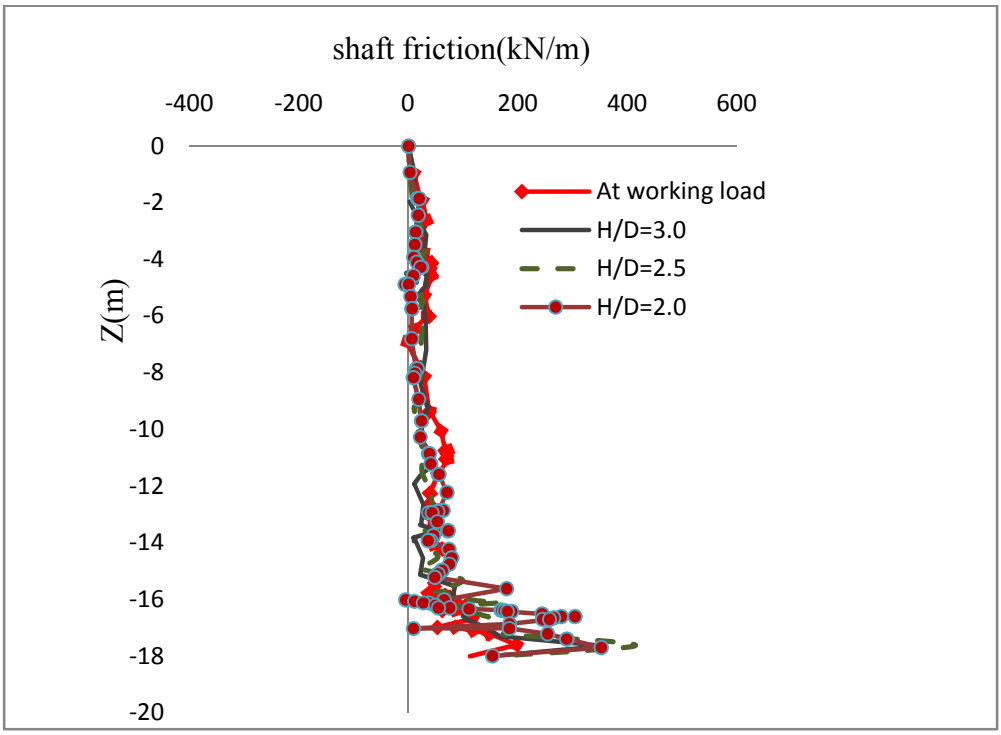

Figure 4-3 Variation of skin friction along the shaft of pile P2

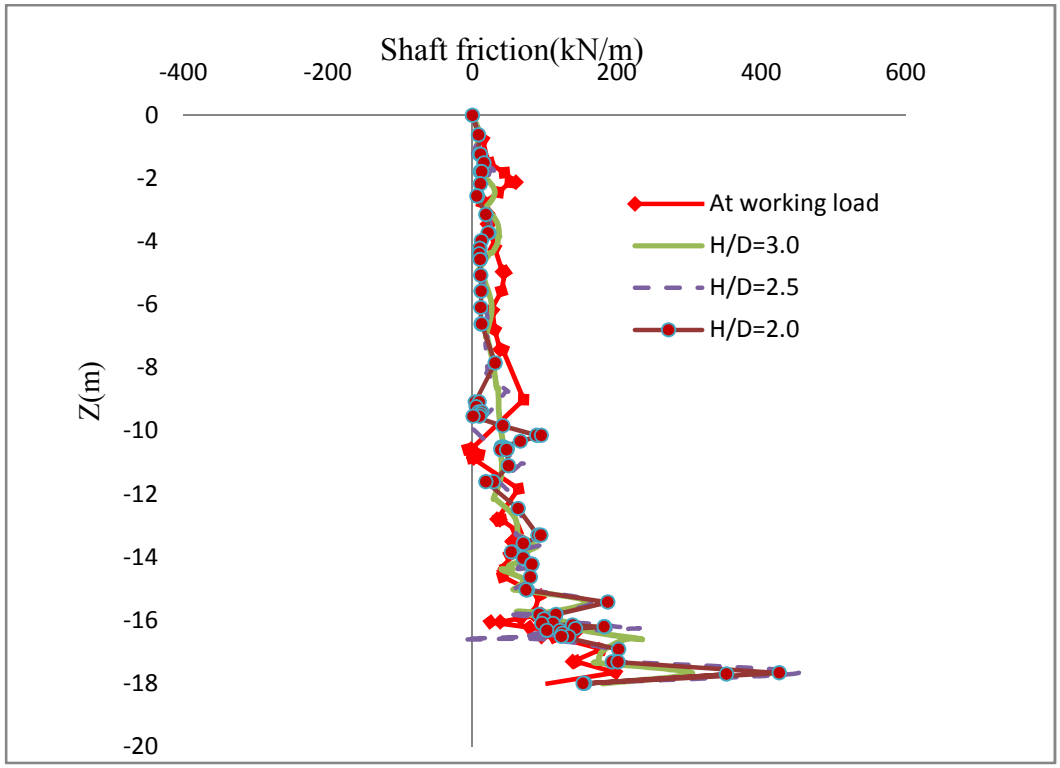

Figure 4-4 Variation of skin friction along the shaft of pile P3

4.5.2 Load Transfer Mechanism of Pile P1, P2 and P3

Variations of load distribution of different piles throughout their length were figure out below (Figure 4.9 to Figure 4.11). This load distribution varies after tunneling because the ground loss establish when tunnel excavation procedure. this ground loss affects the bearing capacity of pile due to stress relief of surrounding soil. Therefore to maintain the pile at equilibrium position loads are transfer from one to the other piles.

As a result, the tunnel excavation near (H/D=2.0) to the skin of pile length load load distribution at the top is decreased and increase at the bottom of pile as shown in pile (p1).however the load distribution of pile (p2) at the top and bottom is increased in addition to that pile (p3) decreases all at the top and the bottom. So load transfer from decreasing part of pile to increasing part and also the other pile of pile group

Table 2.1 Change of load carrying capacity at the top and bottom of pile

H/D=2.0	Head load(kN)	Base load(kN)
P1	-17%	+30%
P2	+21%	+22%
P3	-6%	-2%
H/D=2.5	Head load	Base load
P1	-15%	+15%
P2	+15%	+30%
P3	-2%	+16%
H/D=3.0	Head load	Base load
P1	-8%	-24%
P2	+2%	+70%
P3	+4%	+80%

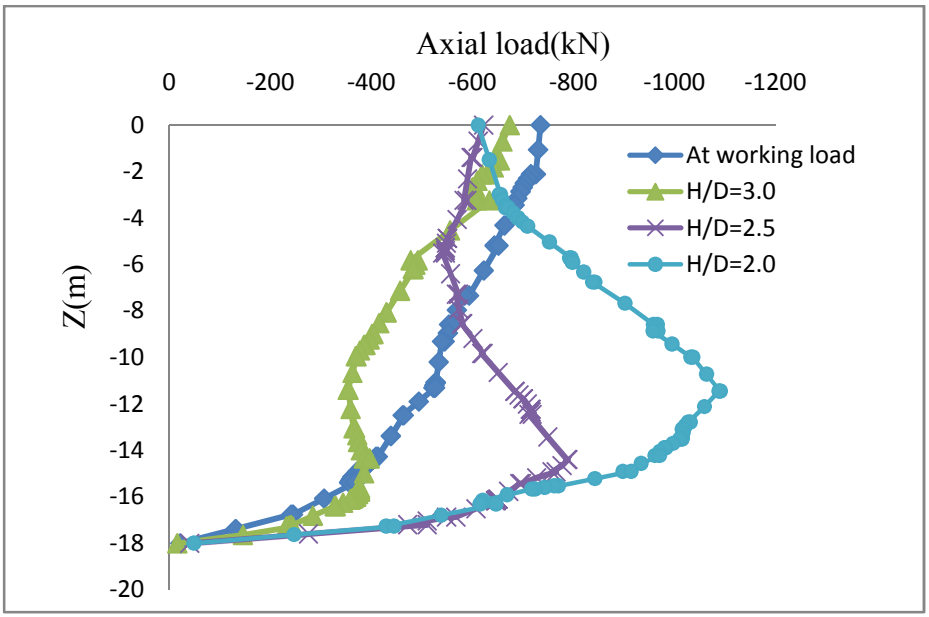

Figure 4-5 Variation of axial load of pile (P1)

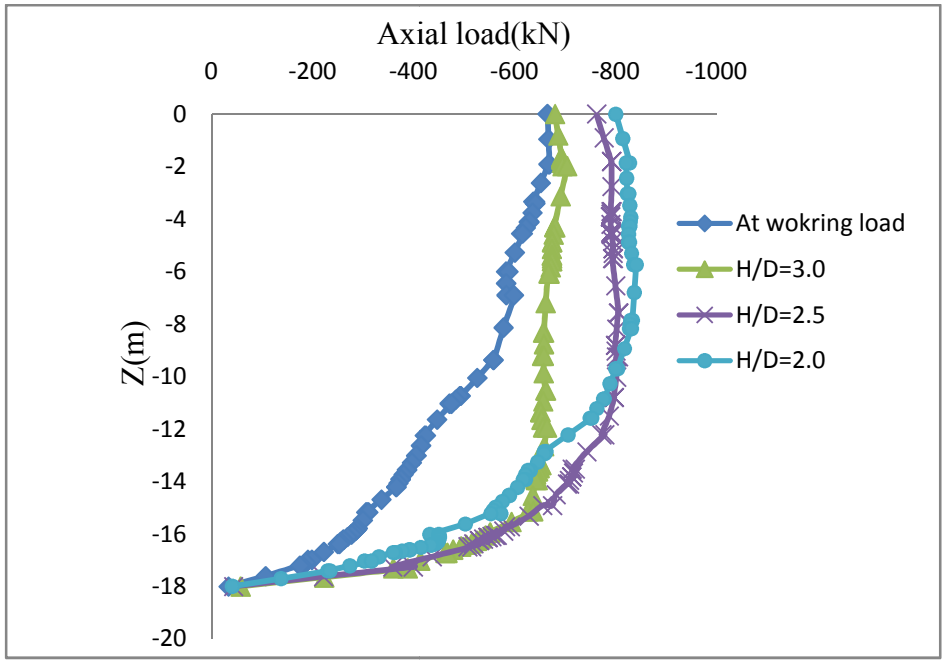

Figure 4-6 Variation of axial load of pile (P2)

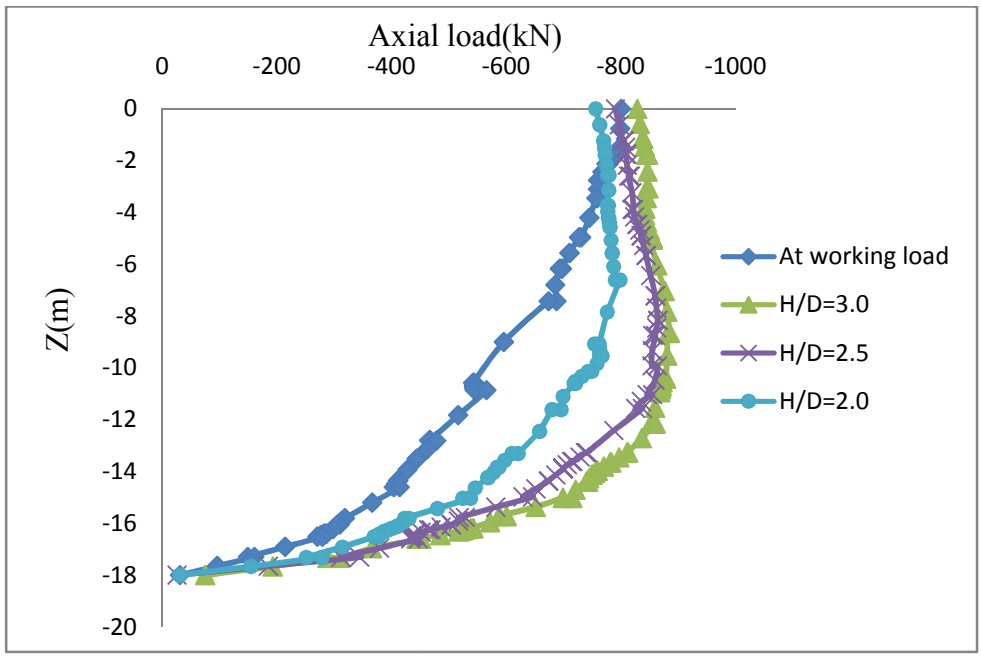

Figure 4-7 Variation of axial load of pile (P3)

4.6 Differential Settlement of Group Pile

In addition to the discussion of pile group settlement in the previous section, differential settlement induced in the pile cap is an important parameter to investigate. During the excavation of nearby pile foundation, as expected, piles closest to the tunnel are subjected to larger ground movement and stress release than those which are farthest from the tunnel excavation. As a result, differential settlement is induced in the piles. Figure 4.11 shows settlements of the piled cup induced at various positions along the width of the pile (see inset in the figure) at different excavation stages (i.e., *H/D*= 2.0, 2.5, and 3.0). The settlement before tunnel advancement (i.e. due to working load) is added in the figure for reference. The settlement occurred in the building was uniform through the width of the pile cap. However, when tunnel advancement was carried out, the pile cup corner closest to the tunnel settled larger than that furthest from the tunnel. In the case of H/D=2.0 the differential settlement was less than the other cases. And also when the tunnel depth increase or near to the pile tip the differential settlement of the foundation is increase. This study shows that piles near to the tunnel settle more than piles far from the tunnel. This cause tilts the supper structure toward the tunnel side. The differential settlement in the pile cap of 3.64, 4.15, and 4.18 mm was induced on completion of excavation stages *H/D*= 2.0, 2.5, and 3.0, respectively The numerical predictions in the previous section showed that the tunnel excavation (advancement) resulted in differential settlement of the pile. This led to tilt the building laterally towards the tunnel excavation.

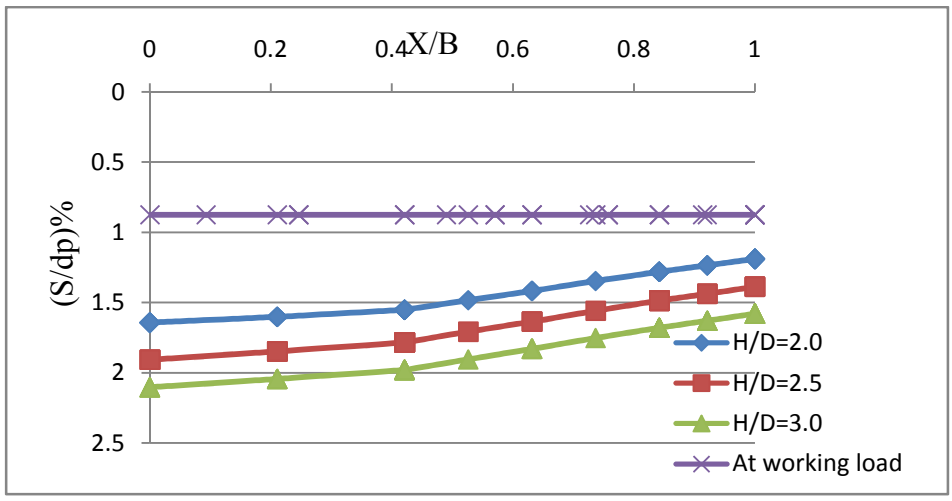

Figure 4-8 Differential settlement in pile cap

CHAPTER FIVE

5 Conclusions and Recommendations

5.1 Conclusions

In this study, a number of numerical analysis were performed that investigates the response of three by three group piles to advanced tunneling in c-ϕ soil and hardening soil constitutive model are used for the soil. The objective of the research was to investigate the response of pile by different mechanisms, in terms of pile head settlement, pile axial load, and skin friction of pile. The following conclusions have been made from this research.

1) Differential settlement of pile cap increases when the tunnels face near 2m to the pile tip. This study shows that piles near the tunnel settle more than piles far from the tunnel. In addition, the tunnel excavation near the pile tip causes a large differential settlement. The differential settlement value in the pile cap is 3.64, 4.15, and 4.18 mm in the case of tunnel position of H/D = 2.0, 2.5, and 3.0, respectively
2) Due to tunnel excavation, additional pile group settlement has occurred. As a result, the group pile is subjected to an additional load of 11.500kN which causes the factor of safety of the group pile to reduce from 3.0 to 1.62.
3) When the tunnel excavation is at H/D=2.0, the skin friction of the pile reduces. However, at H/D=3.0 the tunnel excavation has no significant effect on the skin friction.
4) The surface settlement troughs for three cases of tunnel excavation at the monitoring section (i.e Y/D=0) follows the Gaussians distribution curve.
5) When tunnel excavation is at H/D = 3.0, large pile settlement of the pile group has occurred relative to other tunnel excavations.

5.2 Recommendations

1) In this study the excavation of tunnel advancement consider the ground deformation only due to the volume loss. But when the TBM advancement the vibration of machine causes dynamic effect on the soil and foundation hence this condition shall be considered in the future work.
2) The shape and the dimension of tunnel are constant throughout the analysis. Accordingly parametric studies through varying dimensions and shape shall be incorporated in the future researches.
3) The influence of pile size and spacing is not considered in the thesis. Future study shall incorporate these effects.

References

1. AL-OMARI, RAID RAMZI, AL-SOUD, MADHAT SHAKIR AND AL-ZUHAIRI, OSAMAH IBRAHIM (2019). "Effect of Tunnel Progress on the Settlement of Existing Piled Foundation" Studia Geotechnica et Mechanica, vol.41, no.2, pp.102-113.
2. ATKINSON, J, H AND POTTS, D, M (1979). Subsidence above shallow tunnels in soft ground Journal of Geotechnical Engineering, American Society of Civil Engineers, GT4, pp. 307-325.
3. ATTEWELL, P. B., YEATES, J. & SELBY, A. R. (1986). Soil movements induced by tunneling and their effects on pipelines and structures
4. BRINKGREVE, R., ENGIN, E. & SWOLFS, W. (2013). Plaxis 3D. *Reference Manual*.
5. CHEN, L. T., POULOS, H. & LOGANATHAN, N. (1999). Pile responses caused by tunneling. *Journal of Geotechnical and Geoenvironmental Engineering,* 125**,** 207-215.
6. CHENG, C., DASARI, G., CHOW, Y. & LEUNG, C. (2007). Finite element analysis of tunnel–soil–pile interaction using displacement controlled model. *Tunneling and Underground Space Technology,* 22**,** 450-466
7. CHIANG, K.-H. & LEE, C.-J. (2007). Responses of single piles to tunneling-induced soil movements in sandy ground. *Canadian Geotechnical Journal,* 44**,** 1224-1241..
8. JACOBSZ, S., BOWERS, K., MOSS, N. & ZANARDO, G. (2005). The effects of tunneling on piled structures on the CTRL. *Geotechnical aspects of underground construction in soft ground, Amsterdam***,** 115-122.
9. JACOBSZ, S., STANDING, J., MAIR, R., HAGIWARA, T. & SUGIYAMA, T. (2004). Centrifuge modeling of tunneling near driven piles. *Soils and Foundations,* 44**,** 49-56.
10. KAALBERG, F., TEUNISSEN, E., VAN TOL, A. & BOSCH, J (2005). Dutch research on the impact of shield tunneling on pile foundations. Proceedings of the 5th international symposium on geotechnical aspects of underground construction in soft ground,. Balkema Rotterdam, the Netherlands, 123 -131.
11. LEE, G. T. & NG, C. W. (2005). Effects of advancing open face tunneling on an existing loaded pile. *Journalof Geotechnical and Geoenvironmental Engineering,* 131**,** 193-201.
12. LEE, K., ROWE, R. K. & LO, K. (1992). Subsidence owing to tunneling. I. Estimating the gap parameter. *Canadian Geotechnical Journal,* 29**,** 929-940.

13. LEE, R. (1994). Deformations caused by tunneling beneath a piled structure. *Proc. 13th ICSMFE, New Delhi,India*, 873-878
14. LOGANATHAN, N. & POULOS, H. (1998). Analytical prediction for tunneling-induced ground movements in clays. *Journal of Geotechnical and geoenvironmental engineering,* 124, 846-856. LOGANATHAN, N., POULOS, H. & STEWART, D. 2000. Centrifuge model testing of tunneling-induced ground and pile deformations. *Geotechnique,* 50, 283-294.
15. LOGANATHAN, N, O'CARROLL, J, FLANAGAN, R AND TAN BT (2005). 'EPB TBM tunneling in Singapore old alluvium', Proceedings of the Rapid Excavation and Tunneling Conference, Seattle, Washington, United States, June
16. LOGANATHAN, N AND FLANAGAN, RF (2001). 'Prediction of tunneling-induced ground movements: assessment and evaluation,' Proceedings of the Underground Singapore 2001, Singapore.
17. LOGANATHAN, N, POULOS, HG AND BUSTOS-RAMIREZ, A (2000). 'Estimation of ground loss during tunnel excavation,' paper presented at GeoEng2000, Melbourne, Australia, November
18. LOGANATHAN, N., 2011. *An innovative method for assessing tunnelling-induced risks to adjacent structures*. Parsons Brinckerhoff Incorporated.
19. MAIR, R. & WILLIAMSON, M (2014). The influence of tunneling and deep excavation on piled foundations. Proceedings of the 8th International Symposium on Geotechnical Aspects of Underground.
20. MAIR, R.J. (1993). Developments in geotechnical engineering research: application to tunnels and deep excavations, Unwin Memorial Lecture 1992, Proceedings Institution of Civil Engineers. Civil Engineering, Vol. 93, pp.27-41
21. MORTON, J. & KING, K (1979). Effects of tunneling on the bearing capacity and settlement of piled foundations. Proc. Tunneling,. 57-58.
22. PECK, R, B (1969). Deep excavations and tunneling in soft ground, Proceedings. of 7th International Conference on Soil Mechanics and Foundation Engineering, Mexico City, State-ofthe-art volume, pp. 225-290.

23. SAGASETA, C. (1987). Analysis of undrained soil deformation due to ground loss, Geotechnique 37, pp. 301-320.
24. SELEMETAS, D., STANDING, J. & MAIR, R (2005). The response of full-scale piles to tunneling. Proc. of the Fifth Int. Symposium on Geotechnical Aspects of Underground Construction in Soft Ground, Amsterdam,.
25. SIMPSON B, ATKINSON, J .H AND JOVICIS, V (1996). The influence of anisotropy on calculations of ground settlements above tunnels, Proceedings of International Symposium on Geotechnical Aspects of the Underground Construction in Soft Ground, London preprint vol., pp. 511-514.
26. VERRUIJT, A. & BOOKER, J. (1996). Surface settlements due to deformation of a tunnel in an elastic half plane. *Geotechnique,* 48**,** 709-713
27. VU, M. N., BROERE, W. & BOSCH, J. (2015). Effects of cover depth on ground movements induced by shallow tunneling. *Tunneling and Underground Space Technology,* 50**,** 499-506.

Appendices

Appendix A.1- Soil Constitutive Model

3.2.1 Hardening Soil Model

The Hardening Soil model (HS) is an advanced soil model that is able to obtain more realistic soil response in conditions of non-linearity; it is stress dependency and inelasticity.

The HS model is an elastic-plastic soil model based on the classical plasticity theory (Brinkgreve et al. 2004). For every stress increment, there is a subsequent change of elastic and plastic strain if the soil is undergoing primary loading or only elastic strain if it is under unloading-reloading. The main attraction of this model is its ability to simulate the nonlinear, inelastic and stress dependent behavior of soil.

The model adopts the MC failure criterion.

$$(\sigma_1 - \sigma_3)_f = \left(\frac{2c\prime \cos \emptyset' + 2\sigma' \sin \emptyset'}{1-\sin \emptyset'}\right) \quad (3.1)$$

Figure 3.4 shows the yield surfaces in three-dimensional principle stress space. The hardening law for shear is given in Equation (3.2). For a given shear stress increment, the plastic shear strain increment can be computed from this equation and the corresponding plastic volumetric strain increment can be computed from the flow rule in Equation (3.3). The hardening law for the cap is given in Equation (3.4). For a given increment in mean stress, the plastic volumetric strain increment can be computed using this equation with no shear strain generated

$$f_s = \frac{1}{E_{50}} \frac{q}{1-q/q_u} - \frac{2q}{E_{ur}} - \gamma^p \leq 0 \quad (3.2)$$

$$\Delta\varepsilon_v^p = \sin \psi_m \, \Delta\gamma^p \quad (3.3)$$

$$\Delta\varepsilon_v^p = \frac{\Delta p}{K_c} - \frac{\Delta p}{K_S} = \frac{1}{H} \Delta P \quad (3.4)$$

Where Kc is related to the compression index Cc and Ks is related to the recompression index Cr.

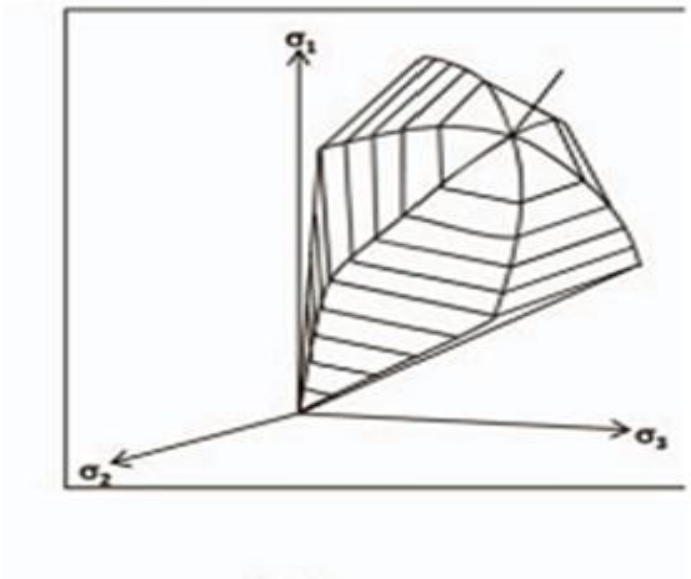

Figure 3-1 Yield surfaces of HS model in 3D

A.1.1. Hardening-Soil Model (Isotropic Hardening)

In contrast to an elastic perfectly-plastic model, the yield surface of a hardening plasticity model is not fixed in principal stress space, but it can expand due to plastic straining. Distinction can be made between two main types of hardening, namely shear hardening and compression hardening. Shear hardening is used to model irreversible strains due to primary deviatoric loading. Compression hardening is used to model irreversible plastic strains due to primary compression in oedometer loading and isotropic loading. Both types of hardening are contained in the present model.

The Hardening-Soil model is an advanced model for simulating the behavior of different types of soil, both soft soils and stiff soils. When subjected to primary deviatoric loading, soil shows a decreasing stiffness and simultaneously irreversible plastic strains develop. The Hardening-Soil model, however, supersedes the hyperbolic model by far. First by using the theory of plasticity rather than the theory of elasticity, second by including soil dilatancy, and third by introducing a yield cap. Some basic characteristics of the model are:

- Stress dependent stiffness according to a power law. Input parameter m
- Plastic straining due to primary deviatoric loading. Input parameter E_{50}^{ref}
- Plastic straining due to primary compression. Input parameter E_{oed}^{ref}

• Elastic unloading / reloading. Input parameters E_{ur}^{ref}

• Failure according to the Mohr-Coulomb model. Parameters c, ϕ and ψ

A basic feature of the present Hardening-Soil model is the stress dependency of soil stiffness. For oedometer conditions of stress and strain, the model implies for example:

$$E_{oed}=E_{oed}^{ref}\ (\sigma/p^{ref})^{m} \qquad \text{A.1.1.1}$$

In the special case of soft soils it is realistic to use m = 1. In such situations there is also a simple relationship between the modified compression index λ^{*}, as used in the PLAXIS Soft Soil Creep model and the oedometer loading modulus.

$$E_{oed}^{ref}=\frac{P^{ref}}{\lambda^{*}} \qquad \text{A1.1.2}$$

$$\lambda^{*}=\frac{\lambda}{1+e_0}$$

Where p^{ref} is a reference pressure. Here It is considered that a tangent oedometer modulus at a particular reference pressure p_{ref}. Hence, the primary loading stiffness relates to the modified compression index λ* or to the standard Cam-Clay compression index λ. Similarly, the unloading-reloading modulus relates to the modified swelling index κ* or to the standard Cam Clay swelling index κ. There is the approximate relationship:

$$E_{ur}^{ref}=\frac{3P^{ref}(1-2V_{ur})}{k^{*}} \qquad \text{A.1.1.3}$$

$$k^{*}=\frac{k}{1+e_0}$$

Again, this relationship applies in combination with the input value m = 1.

A.1.2 Hyperbolic Relationship for Standard Drained Triaxial Test

A basic idea for the formulation of the Hardening-Soil model is the hyperbolic relationship between the vertical strain, ε1, and the deviatoric stress, q, in primary triaxial loading. Here standard drained triaxial tests tend to yield curves that can be described by: (A.1

$$-\varepsilon_1=\frac{1}{2E_{5\ 0}}\ \frac{q}{1-q/q_a} \qquad \text{for :} q< q_f \qquad \text{A.1.2.1}$$

Where *qa* is the asymptotic value of the shear strength

This relationship is portrayed in Figure A.1.1 The parameter E_{50} is the confining stress dependent stiffness modulus for primary loading and is given by the equation

$$E_{50}=E_{50}^{ref}\left(\frac{c\ \cot\varphi-\sigma_3^{'}}{c\ \cot\varphi+P^{ref}}\right)^m \qquad \text{A.1.2.2}$$

Where E_{50}^{ref} is a reference stiffness modulus corresponding to the reference confining pressure p_{ref}. In PLAXIS, a default setting p_{ref} = 100 stress units is used. The actual stiffness depends on the minor principal stress, σ_3', which is the confining pressure in a triaxial test. Please note that σ'_3 is negative for compression. The amount of stress dependency is given by the power m. In order to simulate a logarithmic stress dependency, as observed for soft clays, the power should be taken equal to 1.0. It is suggested that values of m around 0.5 for Norwegian sands and silts. The ultimate deviatoric stress, q_f, and the quantity q_a in A1.1 are defined as:

$$q_f=(c\cot\varphi-\sigma_3')\frac{2\sin\varphi}{1-\sin\varphi} \qquad \text{and:} \qquad q_a=\frac{q_f}{R_f} \qquad \text{A.1.2.3}$$

Again it is remarked that σ'_3 is usually negative. The above relationship for q_f is derived from the Mohr-Coulomb failure criterion, which involves the strength parameters c and ϕ. As soon as q = q_f, the failure criterion is satisfied and perfectly plastic yielding occurs as described by the Mohr-Coulomb model. The ratio between q_f and q_a is given by the failure ratio Rf, which should obviously be smaller than 1. In PLAXIS, R_f = 0.9 is chosen as a suitable default setting. For unloading and reloading stress paths, another stress-dependent stiffness modulus is used:

$$E_{ur}=E_{ur}^{ref}\left(\frac{c\cot\varphi-\sigma_3^{'}}{c\cot\varphi+P^{ref}}\right)^m \qquad \text{A.1.2.4}$$

Where E_{ur}^{ref} is the reference Young's modulus for unloading and reloading, corresponding to the reference pressure pref. In many practical cases it is appropriate to set E_{ur}^{ref} equal to 3 E_{ur} ; this is the default setting used in PLAXIS.

Approximation of Hyperbola by Hardening-Soil Model

To improve convenience, restriction is again made to triaxial loading conditions with $\sigma_2' = \sigma_3'$ and σ_1' being the major compressive stress.

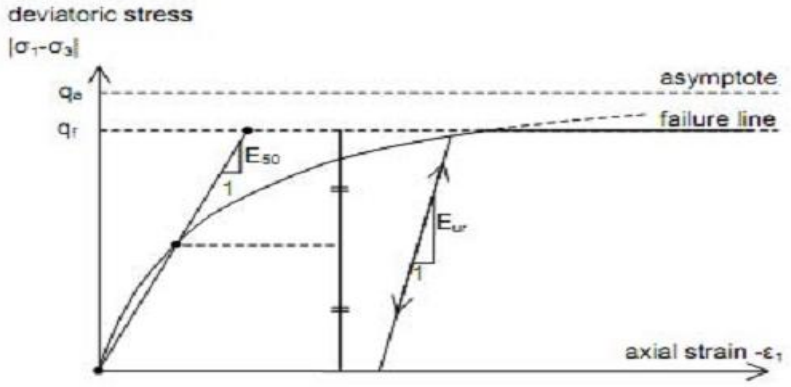

Figure A.1.2.1 Hyperbolic stress-strain relation in primary loading for a standard drained triaxial test

Moreover, it is assumed that q <qf, as also indicated in Figure A.1.2.1 It should also be realized that compressive stress and strain are considered positive. When considering the corresponding plastic strains. This stems from a yield function of the form:

$$f=\overline{f}-\gamma^p \qquad \text{A.1.2.5}$$

Where f is a function of stress and γ^p is a function of plastic strains:

$$\overline{f}=\frac{1}{E_{50}}\frac{q}{1-q/q_a}-\frac{2q}{E_{ur}} \qquad \gamma^p=-\left(2\varepsilon_1^p-\varepsilon_v^p\right)\approx-2\varepsilon_1^p \qquad \text{A.1.2.6}$$

With$q$, qa, E_{50} and E_{ur} as defined by equation (A.1.2.2) to (A.1.2.4) whilst the superscript p is used to denote plastic strains. For hard soils, plastic volume changes (εpv) tend to be relatively Small and this leads to the approximation $\gamma^p \approx -2\varepsilon_1^p$The above definition of the strain hardening parameter γ_p will be referred to later. An essential feature of the above definitions for f is that it matches the well-known hyperbolic law. For checking this statement, one has to consider primary loading, as this implies the yield condition f = 0. For primary loading, it thus yields γ p = f and it follows from Eq. (A.1.2.6) that:

$$-\varepsilon_1^p \approx \frac{1}{2}\overline{f} = \frac{1}{2E_{50}} \frac{q}{1-q/q_a} - \frac{q}{E_{ur}} \qquad \text{A.1.2.7}$$

In addition to the plastic strains, the model accounts for elastic strains. Plastic strainsdevelop in primary loading alone, but elastic strains develop both in primary loading and unloading / reloading. For drained triaxial test stress paths with σ2' = σ3' = constant, the equations:

$$-\varepsilon_1^e = \frac{q}{E_{ur}} \qquad -\varepsilon_2^e = -\varepsilon_3^e = \nu_{ur} \frac{q}{E_{ur}} \qquad \text{A.1.2.8}$$

Where ν_{ur} is the unloading / reloading Poisson's ratio. Here it should be realized that restriction is made to strains that develop during deviatoric loading, whilst the strains that develop during the very first stage of the test are not considered. For the first stage of isotropic compression (with consolidation), the Hardening-Soil model predicts fully elastic volume changes according to Hooke's law, but these strains are not included in (A.1.1.8) For the deviatoric loading stage of the triaxial test, the axial strain is the sum of an elastic component given by (A.1.2.8) and a plastic component according to Eq. (A.1.2.7) Hence, it follows that:

$$-\varepsilon_1 = -\varepsilon_1^e - \varepsilon_1^p \approx \frac{1}{E_{50}} \frac{q}{1-q/q_a} \qquad \text{A.1.2.9}$$

This relationship holds exactly in absence of plastic volume strains, i.e. when $\varepsilon_{pv} = 0$. In reality, plastic volumetric strains will never be precisely equal to zero, but for hard soils plastic volume changes tend to be small when compared with the axial strain, so that the approximation in Eq. (A.1.2.9) will generally be accurate. It is thus made clear that the present Hardening-Soil model yields a hyperbolic stress-strain curve under triaxial testing conditions. For a given constant value of the hardening parameter, γp, the yield condition $f = 0$, can be visualized in p'-q-plane by means of a yield locus. When plotting such yield loci, one has to use Eq. (A.1.2.6) as well as Eqs. (A.1.2.2) and (A.1.2.4) for E_{50} and E_{ur} respectively. Because of the latter expressions, the shape of the yield loci depends on the exponent m. For $m = 1$, straight lines are obtained, but slightly curved yield loci correspond to lower values of the exponent.

Parameters of Hardening-Soil Model

Some parameters of the present hardening model coincide with those of the non hardening Mohr-Coulomb model.

Failure parameter as in Mohr –Coulomb model

C	:(Effective) cohesion	[kN/m^2]
φ	:(Effective) angle of internal friction	[°]
Ψ	:(Effective) angle of internal friction	[°]

Basic parameter for soil stiffness:

E_{50}^{ref}	Secant stiffness in standard drained triaxial test	[kN/m^2]
E_{oed}^{ref}	Primary stiffness for odometer loading	[kN/m^2]
m	power for stress-level dependency of stiffness	[-]

Advanced parameter (it is advised to be used the default setting)

E_{ur}^{ref}	: Unloading and reloading stiffness E_{ur}^{ref}=3E_{50}^{ref}	[kN/m^2]
v_{ur}	: Poisson ration for unloading and reloading (default v_{ur}=0.2)	[-]
p^{ref}	: Reference stress for stiffness (p^{ref}=1000 stress unit)	[kN/m^2]
k_0^{cn}	:k_0=value for normal consideration (default $k_0^{cn}=1-\sin\varphi$)	[-]
p^{ref}	: Failure ratio $^{q_f}/_{q_a}$ (default R^f =0.9) (see figure 4.1)	[-]
$\sigma_{tension}$	: Tensile strength (default $\sigma_{tension}$ =0 stress unit)	[kN/m^2]
$c_{increment}$	: As in Mohr Coulomb model (default $c_{increment}$=0)	[kN/m^2]

The advantage of the Hardening-Soil model over the Mohr-Coulomb model is not only the use of a hyperbolic stress-strain curve instead of a bi-linear curve, but also the control of stress level dependency. When using the Mohr-Coulomb model, the user has to select a fixed value of Young's modulus whereas for real soils this stiffness depends on the stress level. It is therefore necessary to estimate the stress levels within the soil and use these to obtain suitable values of stiffness. With the Hardening-Soil model, however, this cumbersome selection of input parameters is not required. Instead, a stiffness modulus E_{50}^{ref} is defined for a reference minor principal stress of $-\sigma'3= p'^{ref}$ .As a default value, the program uses p^{ref}= 100 stress units.

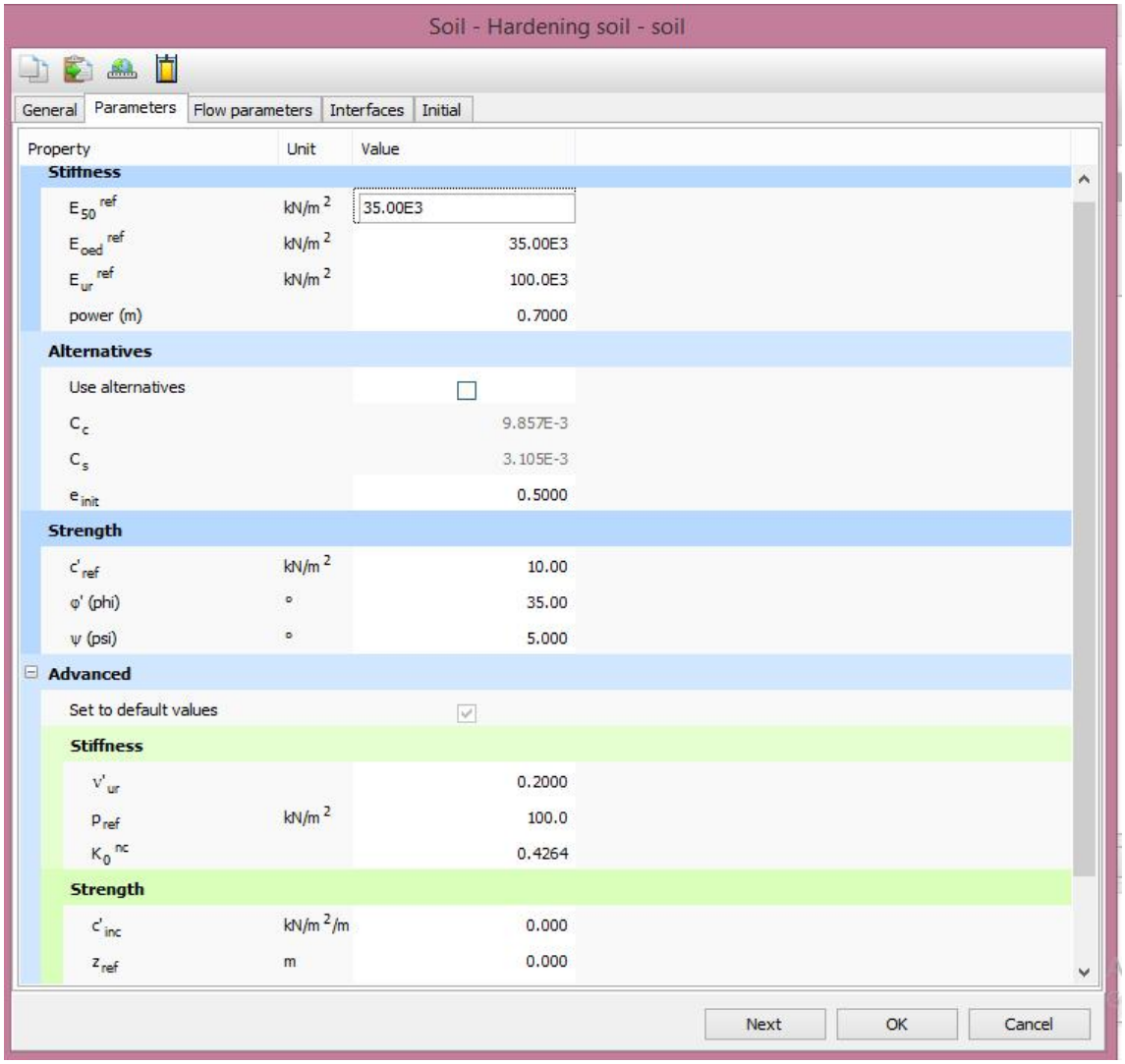

Figure A.1.2.2Basic parameters for the Hardening-Soil model

Within Hooke's theory of elasticity conversion between E and G goes by the equation $E = 2\ (1+\nu)\ G$. As E_{ur} is a real elastic stiffness, one may thus write $E_{ur} = 2\ (1+\nu)\ G_{ur}$, where G_{ur} is an elastic shear modulus. PLAXIS allows for the input of E_{ur} and ν_{ur} but not for a direct input of G_{ur}. In contrast to E_{ur}, the secant modulus E_{50} is not used within a concept of elasticity. As a consequence, there is no simple conversion from E_{50} to G_{50}. In contrast to elasticity based models, the elasto plastic Hardening-Soil model does not involve a fixed relationship between the (drained) triaxial stiffness $E_{50}$and the odometer stiffness E_{oed} for one-dimensional

compression. Instead, this stiffness can be inputted independently. Having defined E_{50} by Eq. (A.1.2.2) it is now important to define the oedometer stiffness. Here we use the equation:

$$E_{oed}=E_{oed}^{ref}\left(\frac{c\cot\varphi-\sigma_3^{'}}{c\cot\varphi+P^{ref}}\right)^{m}$$

Where E_{oed} is a tangent stiffness modulus as indicated in Figure (A.1.4). Hence, E_{oed}^{ref} is tangent stiffness at a vertical stress of .$\sigma'_1 = p^{ref}$.

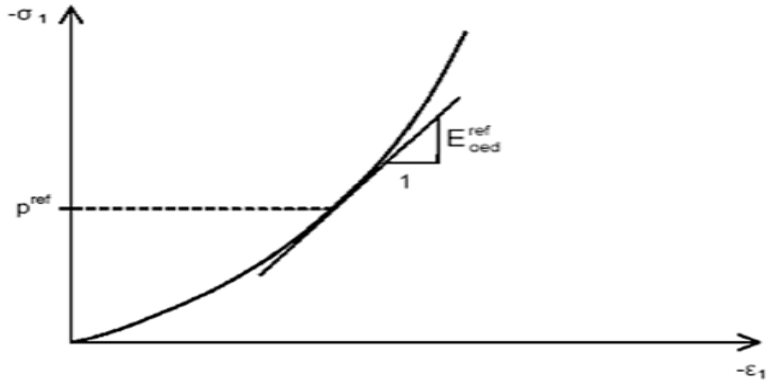

Figure A.1.2.3 Definition of E_{oed} in oedometer test result

Appendix A.2Shading Profiles of Out Puts

1. Tunnel level of excavation in (H/D=2.0) and the phase of excavation in the middle of pile group

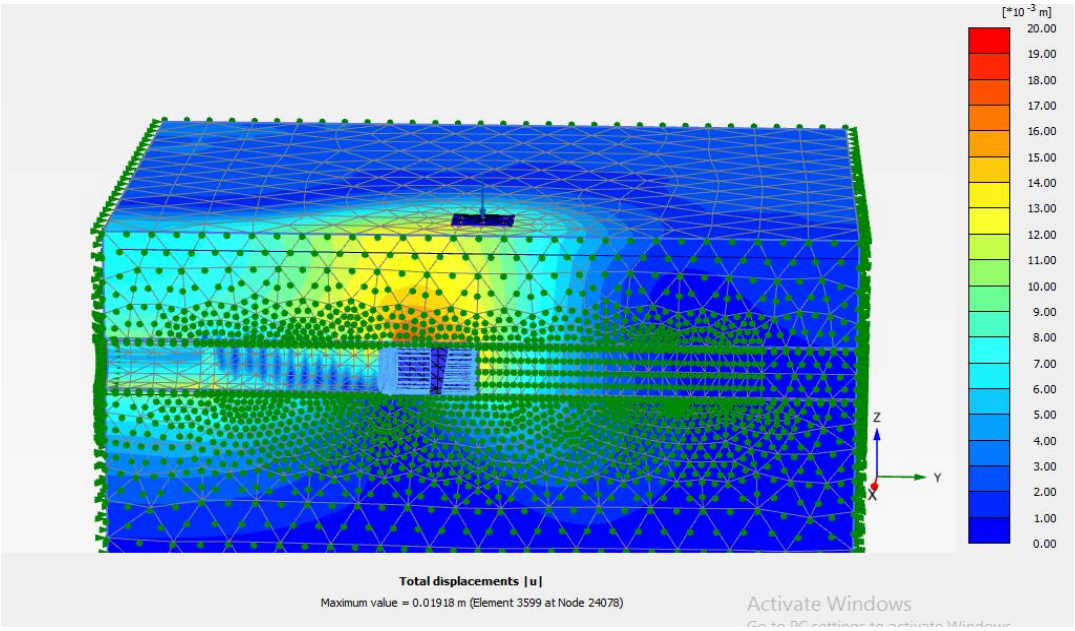

2. Tunnel level of excavation in (H/D=2.0) and the phase of excavation in the beyond the pile group

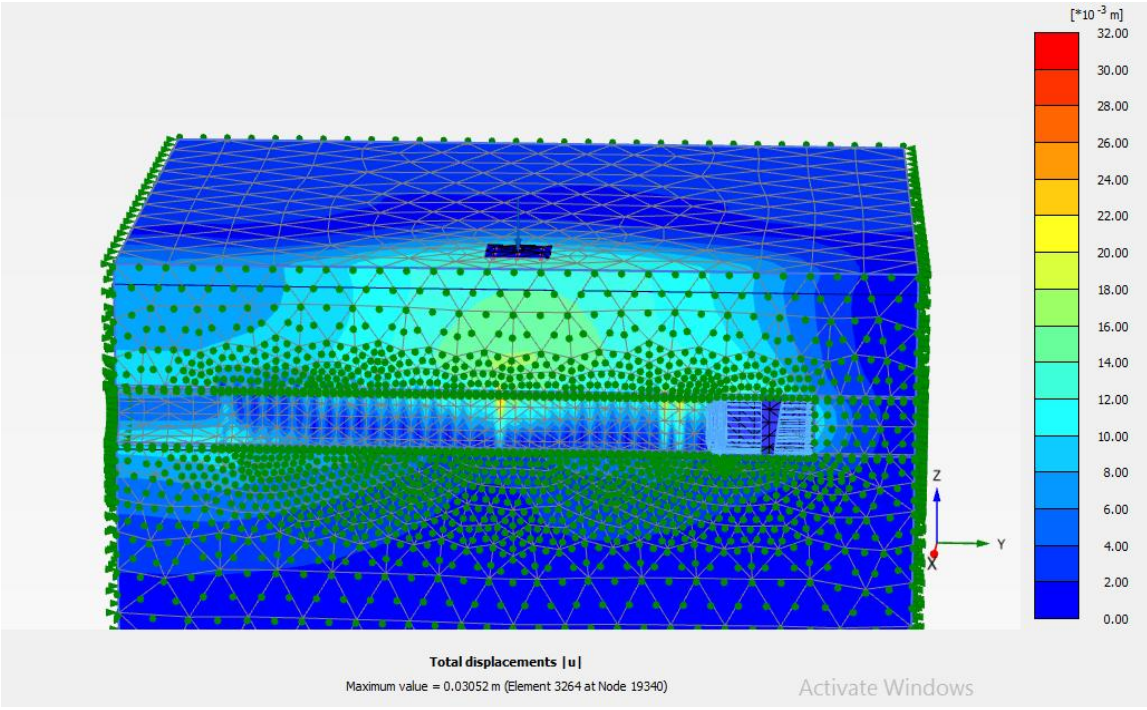

3. Tunnel level of excavation in (H/D=2.5) and the phase of excavation in the middle of pile group

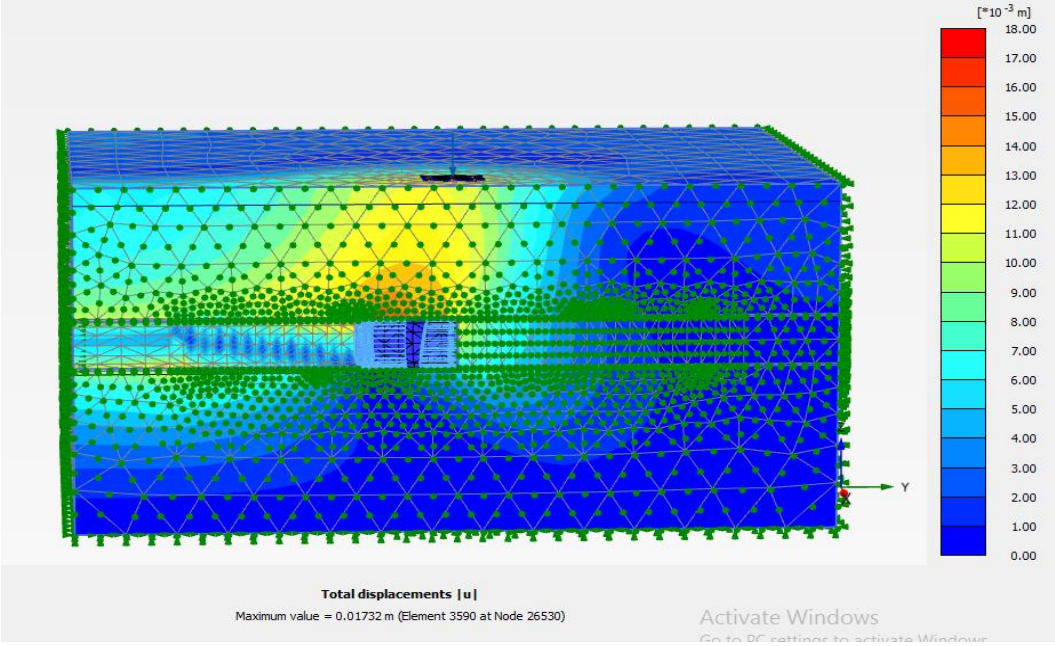

4. Tunnel level of excavation in (H/D=2.5) and the phase of excavation in the beyond the pile group

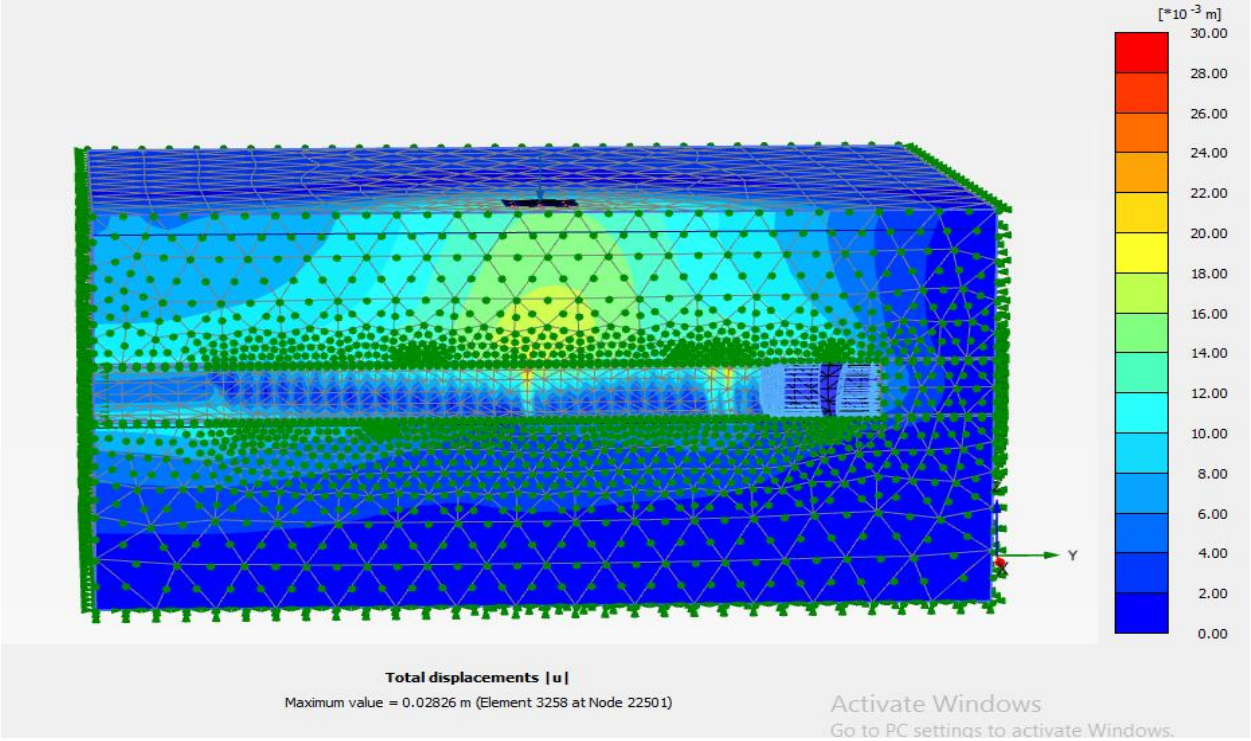

5. Tunnel level of excavation in (H/D=3.0) and the phase of excavation in the middle of pile group

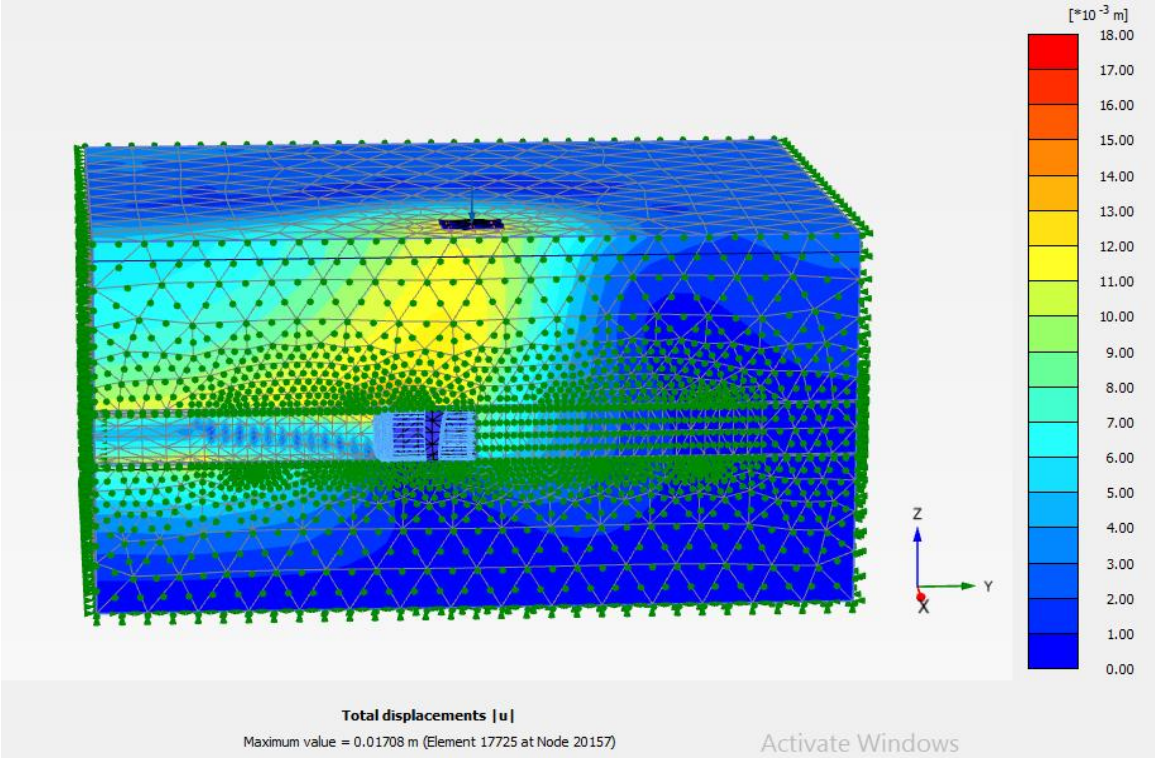

6. Tunnel level of excavation in (H/D=3.0) and the phase of excavation in the beyond the pile group